On Fractional Differential Equations: The generalised Cattaneo equations

Sahooda Valla

0005162Y

Supervisor: Prof. E. Momoniat

A dissertation submitted to the Faculty of Science, University of the Witwatersrand, Johannesburg, in fulfillment of the requirements for the degree of Master of Science

DECLARATION

I declare that this dissertation is my own unaided work. It is being submitted for the degree of Masters of Science at the University of the Witwatersrand, Johannesburg. It has not been submitted before for any degree or examination at any other university.

Sahooda Valla

March 3, 2009

ABSTRACT

The aim of this dissertation is to determine numerical solutions to fractional diffusion and fractional Cattaneo equations using finite difference formula and other defined schemes. The spatial derivatives and time derivatives of integer order are approximated by a finite difference approximation. Spatial derivatives of fractional order are approximated using the Grünwald formula. Fractional time derivatives are approximated using the Grünwald-Letnikov definition of the Riemann-Liouville fractional derivative. The resulting difference schemes are evaluated using Mathematica.

The results obtained show that the fractional Cattaneo equaions have propagation and diffusive properties. When the fractional exponent is 0.1 with the diffusivity coefficient being greater than 0.1 one obtains numerical results that are unstable and display oscillatory behaviour. For other combinations of values, numerical results are stable and consistent with diffusive behaviour.

ACKNOWLEDGEMENTS

Thank you to supervisor Professor Ebrahim Momoniat for his patience and support.

DEDICATION

This dissertation is dedicated to Mr. and Mrs. Valla. As well as to Inez Valla and Charles Walters. Thank you for all the motivation and never ending support.

Contents

List of Figures

1 Introduction

This chapter serves to provide an overview of anomalous diffusion. It provides an introduction to the Cattaneo equations and looks briefly at the application of fractional derivatives in finance.

1.1 Overview

Diffusion is the net movement of particles from an area of higher concentration to an area of lower concentration, i.e. down a concentration gradient. We say the net movement because the diffusing particles move randomly between the areas of higher and lower concentration.

Since there are more particles present in the higher concentrated area, more particles leave this area than the lower concentrated area (Figure 1). The concentration gradient, which is rather high at first, gradually decreases while the concentration difference reduces, i.e. until the system reaches equilibrium.

This definition is based on the movement of particles. As an example of demonstrating diffusion consider a drop of dye placed in a glass of water (Figure 2). At first the drop is observed clearly as a drop. We can say that the concentration of dye in that droplet is higher compared to the surrounding water particles.

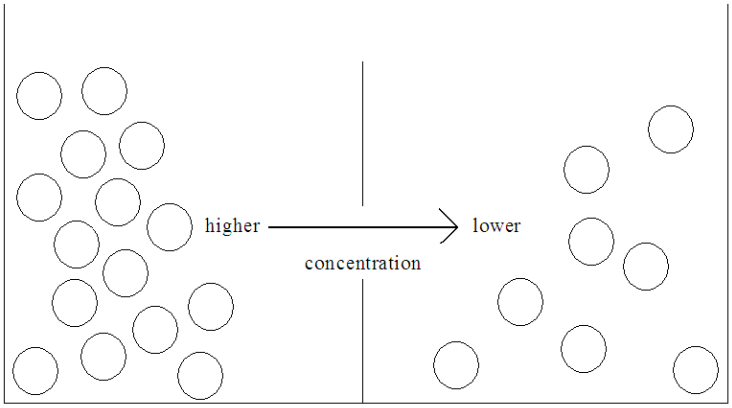

Figure 1: Diffusion of particles down a concentration gradient; from an area of higher concentration to an area of lower concentration.

After a period of time has elapsed the whole glass of water is of a uniform colour - that of the dye. The dye particles have diffused throughout the medium (the water), until they are evenly dispersed amongst the water molecules.

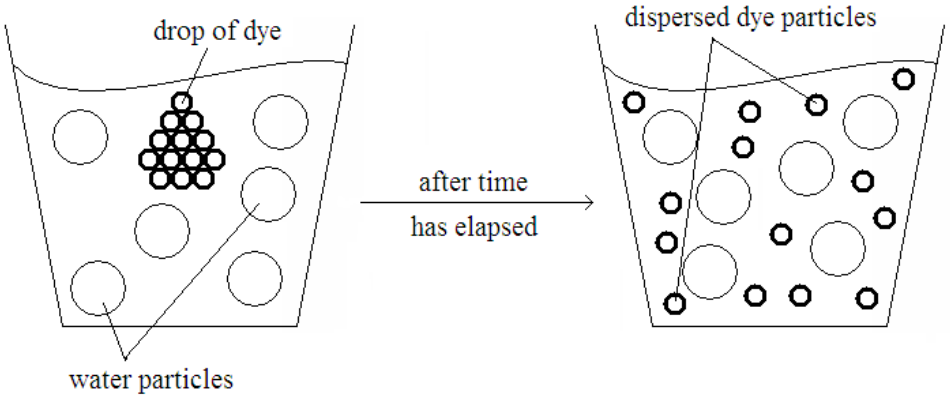

Figure 2: Example of the diffusion of dye particles in water.

This definition is analogous to the diffusion of heat. Consider a thin circular rod of length L and cross-sectional area A (Figure 3). We refer to the derivation presented by Zill and Cullen [14] of the diffusion equation when we suppose the following:

- the rod coincides with the x-axis on the interval $[0, L]$,

- flow of heat within the rod takes place in the x-direction only,
- the lateral and curved surfaces of the rod are insulated,
- no heat is being generated within the rod, and
- the diffusion coefficient is constant.

Zill and Cullen [14] use two empirical laws of heat conduction

$$Q = \gamma m u, \tag{1.1}$$

the quantity of heat Q in an element of mass m where u is the temperature and

$$Q_t = -kAu_x, \tag{1.2}$$

the rate of heat flow Q_t through the cross-section is proportional to the area A of the cross-section and the rod with respect to x of the temperature where the "$-$" represents heat flow in the direction of decreasing temperature.

If the cross-section of the rod between x and Δx is very thin then $u(x,t)$ is the approximate temperature at each point in the interval $[0, L]$. If the mass of the cross-section is $m = \rho(A\Delta x)$, we can substitute this into equation (1.1) to obtain

$$Q = \gamma \rho A \Delta x u(x,t). \tag{1.3}$$

Heat flows in the x-direction and builds up in the cross-section at a net rate

$$-kAu_x(x,t) - [-kAu_x(x+\Delta x,t)] = kA[u_x(x+\Delta x,t) - u_x(x,t)] \tag{1.4}$$

(energy is conserved). Differentiating equation (1.3) with respect to t we obtain

$$Q_t = \gamma\rho A\Delta x u_t(x,t). \tag{1.5}$$

Combining equations (1.2), (1.4) and (1.5) we obtain

$$\begin{aligned} \gamma\rho A\Delta x u_t(x,t) &= -kA(u_x(x,t) - u_x(x+\Delta x,t)) \\ \Rightarrow u_t(x,t) &= (k/\gamma\rho)(1/\Delta x))(u_x(x+\Delta x,t) - u_x(x,t)). \end{aligned} \tag{1.6}$$

We take the limit of (1.6) as Δx approaches 0. This yields the diffusion equation $u_t(x,t) = Du_{xx}(x,t)$, where $D = (k/\gamma\rho)$ is the diffusivity constant. We fix the temperature at the end of the rod giving the boundary condition $u(-\infty,t) = u(\infty,t) = 0$

Diffusion of heat is the flow of heat along the rod, from the end where heat is being transferred, throughout the length of the rod. The diffusion of heat occurs down a temperature gradient, i.e. heat moves along the rod from an area of higher temperature to an area of lower temperature.

When heat is transferred to the rod, energy is being transferred to the particles of the rod. This excites the particles, causing them to vibrate. The particles collide with each other, randomly transferring energy to the next particle. In turn this particle vibrates and transfers energy to the next. As energy is being transferred each particle experiences a decrease in its energy. Heat energy can be transferred randomly between the higher and lower temperature area but the net movement down a temperature gradient is maintained.

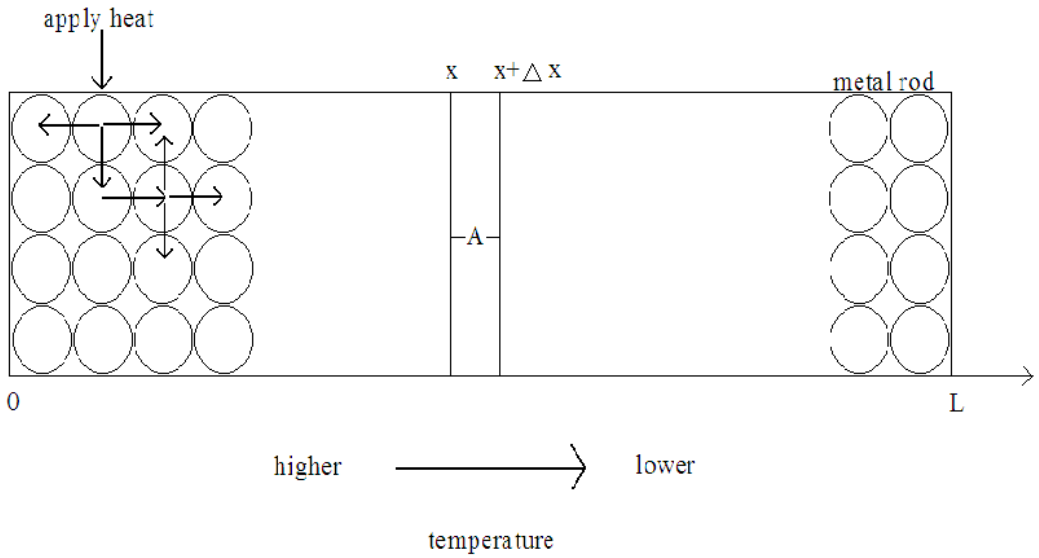

Figure 3: Example illustrating diffusion of heat along a thin rod of length L and cross-sectional area A.

This random movement of particles is called anomalous (anomalous meaning irregular) diffusion and is found in many real world systems such as chemical processing, polymers, in financial modeling and in the transport of fluids in porous media. This diffusion process can be reduced to analysing solutions of the phenomenological diffusion equation

$$\partial_t u(x,t) = D u_{xx}(x,t), \tag{1.7}$$

where $u(x,t)$ denotes the concentration or temperature of the diffusing material and D is the diffusivity constant. D depends on the diffusing material and the medium it is diffusing through.

The mechanism of diffusion is Brownian motion. Einstein and Brown did extensive work on Brownian motion. In Einstein's first paper on Brownian motion [17] he predicts that the root mean squared displacement (λ_x) of suspended particles is proportional to the square root of time i.e. $\lambda_x = \sqrt{2Dt}$ (D is the diffusivity coefficient).

Brownian motion is the simplest continuous-time stochastic process and is also described as the random movement of particles. Each particle collides with its neighbouring particles. Due to this the motion of a particle is characterised by a mean free path which tends to confine the particle. However, the particle is not restored to its original position [20] and is therefore still free to move about in the diffusing medium.

The mathematical model for Brownian motion has real world applications such as the fluctuations in the stock market [24]. Brownian motion has played an important role in the interpretation of statistical physics.

Continuous time random walks can be coupled with Brownian motion and fractional calculus to provide an improved estimate in modeling anomalous diffusion. A random walk is a stochastic process defined as a mathematical formalization of a trajectory where successive steps are taken in random directions. It represents the probability distribution function of the position of a particle at a certain time which depends on the particles' position at the previous time

and a probability rule for its subsequent step length and direction. The smaller the step size, the closer an approximation a random walk (which is a discrete fractal) is to Brownian motion (which is a true fractal) [5].

A continuous time random walk is a stochastic process involving a particle taking a step or making a jump of random lengths separated by periods of rest of random lengths. It is characterised by a probability distribution function to find a random walker at a certain position and a certain time if it started from the origin and at time equal to zero [5, 11]. Hence continuous time random walks are random walks governed by two probability distribution functions, one for the step length and the other for the waiting time distribution [11, 21]. As mentioned by Lin and Xu [30], continuous time random walk schemes are considered in the derivation of time-fractional differential equations.

When it comes to modeling anomalous diffusion processes fractional calculus is considered a powerful mathematical tool. Fractional differential equations underlie random walks and fractional Brownian motion and have many applications in finance, computational biology and acoustics [10, 27].

If α is a fraction then $\partial^\alpha/\partial t^\alpha$ mirrors the anomalous waiting time distribution and $\partial^\alpha/\partial x^\alpha$ mirrors a power-law step length distribution [35]. Lin and Xu [30] also note that the fractional derivative

represents a degree of memory in the diffusing material. This is because the whole information of the function is accumulated in a weighted form. In simpler terms the solution of the probability distribution function $u(x,t)$ at a certain time within its time interval depends on the solutions of $u(x,t)$ at all the previous time levels. This is known as the memory effect.

Anomalous transport processes [42] are characterised by the mean-square displacement (MSD) of the form

$$\left\langle x^2(t) \right\rangle \propto t^{\gamma}. \tag{1.8}$$

This is due to fractional equations predicting the non-linear increase of the variance of the distance traveled at a time t [49]. From equation (1.8) γ is the anomalous diffusion exponent where if $0 < \gamma < 1$ we have subdiffusion, if $\gamma = 1$ we have normal diffusion and if $1 < \gamma < 2$ we have superdiffusion. The MSD gives us an idea of the rate of diffusion of the random walker [5, 12, 44, 49].

In anomalous diffusion particles spread at a rate inconsistent with the classical Brownian motion model [1, 34]. Lynch *et al* [44] state that anomalous diffusion may be a consequence of particles being trapped in certain positions along a trajectory; this is termed subdiffusion and is a process that is slower than normal diffusion. If it is a case of jets of particles along a trajectory it is termed superdiffusion or enhanced diffusion, where in this process diffusion occurs faster than what the classical model predicts.

Fick's law is equivalent to an equation of motion and the inertial force that is required by Newton's second law is neglected [32]. Brownian motion is used to approximate the movement of particles. This is an abstract concept since the length of the process is infinite and no particle can move an infinite distance in a finite space of time [17]. Mathematically speaking, the diffusion equation (1.7) is a parabolic partial differential equation. These factors lead to the anomalous properties typical of the phenomenological diffusion equation. By this we mean that equation (1.7) models infinite speeds of propagation.

As a simple example in the diffusion of heat, a sudden change in temperature made at some point in a body will be felt instantly everywhere in the body. This is not physical as heat propagates in a finite time in a finite domain. Joseph and Preziosi [22, 23] indicate that the diffusion equation is correct only after a sufficiently long time has passed [18, 19].

The diffusion equation has limited applicability to real systems, [32] in which anomalous diffusion is present. Examples where it is present are the percolation of gases, the standard solid-on-solid model for surface growth and the propagation of thin liquid films under gravity [27].

1.2 The Cattaneo equations

Carlo Cattaneo [9] was the first to build an explicit mathematical theory to correct the non-physical property of infinite propagation of the Fourier and Fickian theory of the diffusion of heat [6].

In 1948 Cattaneo replaced the constitutive equation $J(x,t) = -Du_x(x,t)$ by

$$J(x,t) + \tau \partial_t J(x,t) = -Du_x(x,t) \tag{1.9}$$

to correct the non-physical property of infinite speeds admitted by parabolic diffusion equations. The change in the constitutive equation (1.9) yields a hyperbolic diffusion equation or Cattaneo's equation:

$$\partial_t u(x,t) + \tau \partial_t^2 u(x,t) = Du_{xx}(x,t), \tag{1.10}$$

where τ is a characteristic relaxation time constant and $\tau \ll 1$.

The definition of the relaxation time is given as the time required for a system to respond to a change by well-defined external stimuli and to reach equilibrium. For example until the dye particles have diffused throughout the water, or the particles of the rod slowing down as energy is passed on from the faster to the slower moving particles.

As a result of the change, equation (1.10) describes diffusion processes with finite speeds of propagation. The Cattaneo equation (1.10) is also known as a telegraph equation. The telegraph equation is the simplest mathematical model combining waves and diffusion.

Cattaneo's equation has many applications and is used extensively in the theory of viscoelastic fluids and solids, relaxing gas dynamics, irreversible thermodynamics, cosmological models, finance modeling, and in the theory of diffusion in crystalline solids. However, the Cattaneo equation lacks the ability to capture ballistic transport processes [8, 9].

Compte and Metzler [12] generalise the Cattaneo equation (1.10) by introducing fractional derivatives with a CTRW (continuous time random walk) scheme. In doing so the generalised Cattaneo equation now describes anomalous transport processes. An introduction of a fractional derivative and an *ad hoc* generalisation of the continuity equation $\partial_t u(x,t) = -J_x(x,t)$ relaxes the flux to give

$$\partial_t^\gamma u(x,t) = -J_x(x,t). \tag{1.11}$$

Combining this with the modified constitutive equation

$$J(x,t) + \tau^\gamma \partial_t^\gamma J(x,t) = -D u_x(x,t), \tag{1.12}$$

we obtain one form of the generalised Cattaneo equation (GCE)

$$\partial_t^\gamma u(x,t) + \tau^\gamma \partial_t^{2\gamma} u(x,t) = D u_{xx}(x,t) \qquad \text{(GCE I)}, \tag{1.13}$$

where the Riemann-Liouville definition of the fractional derivative [40] is:

$$\partial_t^\gamma u(x,t) = {}_0D_t^\gamma u(x,t) = \frac{1}{\Gamma(1-\gamma)} \frac{\partial}{\partial_t} \int_0^t dt' \frac{u(x,t')}{(t-t')^\gamma} \qquad \text{for} \quad 0 < \gamma < 1. \tag{1.14}$$

The introduction of τ^γ in equation (1.13) keeps the dimensions in order. The fractional derivative in equation (1.14) is described as a

non-local operator as its value depends on the entire function $u(x,t)$ and is thus used in modeling path dependent phenomena. Other references that may be consulted are [15, 16, 25, 31, 36, 40].

This is one generalisation. There are two other generalisations proposed by Compte and Metzler [12] where their derivations are explained which have the form:

$$\partial_t^{2-\gamma} u(x,t) + \tau^\gamma \partial_t^2 u(x,t) = D u_{xx}(x,t), \qquad \text{(GCE II)} \qquad (1.15)$$

$$\partial_t^{\gamma} u(x,t) + \tau \partial_t^{1+\gamma} u(x,t) = D u_{xx}(x,t). \qquad \text{(GCE III)} \qquad (1.16)$$

In essence these generalisations are equivalent as they describe anomalous diffusion processes with a finite velocity of propagation.

Exact analytical solutions cannot be found for most nonlinear fractional differential equations. However, we refer to work that applies the Adomian decomposition method [36, 38, 46] to obtain approximate analytical solutions. The Adomian decomposition approach adds the value of providing immediate and visible symbolic terms of analytical solutions, where the solution takes the form of a convergent series.

1.3 Application to finance

Financial markets trade a variety of securities such as foreign exchange, equities, bonds, swaps and forwards. These are a few examples of derivatives. Derivatives are financial instruments that derive their value from an underlying asset or stock price S_t.

When modeling trading derivatives, arbitrage possibilities need to be taken into account. It also interesting to note that modeling the prices requires modeling an entire curve over time. A common model used is the classical Black-Scholes (BS) pricing model proposed by Black, Scholes and Merton [33, 24, 43]. In this model there are two assets being traded continuously over a time interval $[0, T]$.

The BS model:

$$d(\ln S_t) = (\mu - \frac{1}{2}\sigma^2)dt + \sigma dB_t \tag{1.17}$$

where $\ln S_t$ follows a random walk, μ is the average compounded growth of the stock S_t, dB_t is the increment of Brownian motion which has a Gaussian distribution and $\sigma \geq 0$ is defined as the volatility of the returns from holding S_t.

The BS model, being a geometric Brownian motion model for a stock, is a volatile model and therefore not suitable for many markets. An improved approach to modeling is rather to make use of fractional Brownian motion. The incorporation of a Lévy random walk process into the stock price is another approach to overcome the short-comings of the BS model. There are three main models in this area: the LS (Lévy stable) model, the CGMY (CarrGeman-MadanYor) model and the KoBoL (a Lévy process studied by Koponen, Boyarchenko, and Levendorskii) model. These models can be rewritten using fractional derivative operators.
By making use of a Lévy process to derive a model we are actually

using a combination of two independent processes, namely Brownian motion (also considered as the stochastic component) and a jump component.

Madan *et al* [39] introduce the term jump-diffusions to describe asset returns. What is meant by this term is that diffusion and jumps (from random walks performed by a random walker or particle or, in this case, stock price) are important in modeling asset returns. The role played by diffusion is the capture of frequent but small moves, whereas jumps capture the rare but large moves of the random walker. In other words we can say that over a time step Δt the stock price S_t can diffuse or jump to values such as $S_{t+\Delta t}$ which may not necessarily be close to the initial value S_t.

Instead of looking at the localized information about the underlying asset, fractional derivatives weigh the information over a range of values of the underlying asset. In terms of the BS model (1.17) the jump of a random walker represents the log-returns of the stock price and the waiting time distributions measure the delay between transactions.

The price of a European-style option (the simplest type of derivative) for the BS model satisfies a partial differentiation equation. If r is the risk-free rate the equation is

$$\frac{\partial V(S,t)}{\partial t} + \frac{1}{2}\sigma^2 S^2 \frac{\partial^2 V(S,t)}{\partial S^2} + rS\frac{\partial V(S,t)}{\partial S} = rV(S,t). \qquad (1.18)$$

If we make the substitution $x = \ln S_t$ equation (1.18) can be written as the diffusion equation

$$\frac{\partial V(x,t)}{\partial t} + \frac{1}{2}\sigma\frac{\partial^2 V(x,t)}{\partial x^2} + (r - \frac{1}{2}\sigma^2)\frac{\partial V(x,t)}{\partial x} = rV(x,t). \quad (1.19)$$

As previously mentioned this model has certain drawbacks which are overcome by using a Lévy process and fractional derivatives. Fractional partial differential equations are used extensively by stochastic modelers because of their generality and the link their solutions give to almost all stable distributions such as Lévy distributions. Other references provide extensive detail [24, 26, 28, 29, 33, 43].

Álvaro Cartea and Diego del-Castillo-Negrete [2] explain how Lévy processes are incorporated in derivative pricing and the use of fractional derivative operators. They look at the three models mentioned namely LS, CGMY and KoBoL. However, the fractional partial differential equations all have the standard form

$$\begin{aligned}\frac{\partial V(x,t)}{\partial t} + A(x)\frac{\partial V(x,t)}{\partial x} + B(x)\frac{\partial^\alpha (f(x)V(x,t))}{\partial_+ x^\alpha} \\ +C(x)\frac{\partial^\alpha (h(x)V(x,t))}{\partial_- x^\alpha} + D(x)V(x,t) = 0.\end{aligned} \quad (1.20)$$

The left-shifted Grünwald formula

$$\frac{\partial^\alpha (h(x)V(x,t))}{\partial_- x^\alpha} = \frac{1}{\Gamma(-\alpha)}\lim_{N\to\inf}\frac{1}{h^\alpha}\sum_{k=0}^{N}\frac{\Gamma(k-\alpha)}{k+1}f(x+(k-1)h)V(x+(k-1)h,t)$$

can be used to approximate $\dfrac{\partial^\alpha (h(x)V(x,t))}{\partial_- x^\alpha}$.

The right-shifted Grünwald formula

$$\frac{\partial^\alpha (h(x)V(x,t))}{\partial_+ x^\alpha} = \frac{1}{\Gamma(-\alpha)} \lim_{N\to \inf} \frac{1}{h^\alpha} \sum_{k=0}^{N} \frac{\Gamma(k-\alpha)}{k+1} f(x-(k-1)h)V(x-(k-1)h,t)$$

can be used to approximate $\dfrac{\partial^\alpha (f(x)V(x,t))}{\partial_+ x^\alpha}$.

This dissertation applies finite difference techniques to fractional diffusion equations (where the fractional derivative operates on the spatial variable) and fractional Cattaneo equations (where the fractional derivative operates on the time variable). The numerical solutions are presented graphically, displaying the behaviour of the solutions over time.

This dissertation is set up as follows. Chapter 2 discusses the derivation of the phenomenological diffusion equation, as well as the Cattaneo equations. The last section of Chapter 2 discusses the numerical schemes for solving the fractional differential equations. Chapters 3 and 4 apply the discussed schemes to the different fractional diffusion and fractional Cattaneo equations. Conclusions and possible future work are given in Chapter 5.

2 Derivation of equations and numerical schemes through discretization

In this chapter we look at the derivations of the phenomenological diffusion equation, the Cattaneo equation and the first (GCE I), second (GCE II) and third (GCE III) generalised Cattaneo equations [12]. These generalisations are supported by different schemes (continuous time random walks, non-local transport theory, and delayed flux-force relation as described by Compte and Metzler [12]) and are thus derived differently. The last section gives a brief description on the discretization used in formulating the numerical schemes for the equations we wish to solve. The definition of the initial condition is also given.

2.1 The phenomenological diffusion equation

The phenomenological diffusion equation can be derived by substituting Fick's first law [12, 13] (which describes steady-state diffusion)

$$J(x,t) = -Du_x(x,t), \tag{2.1}$$

into the mass balance equation

$$\partial_t u(x,t) = -J_x(x,t). \tag{2.2}$$

Differentiating (2.1) with respect to x we get

$$\frac{\partial J(x,t)}{\partial x} = -D\frac{\partial^2 u(x,t)}{\partial x^2}. \tag{2.3}$$

Substituting (2.3) into (2.2) yields

$$\frac{\partial u(x,t)}{\partial x} = -\left(-D\frac{\partial^2 u(x,t)}{\partial x^2}\right). \tag{2.4}$$

Simplifying (2.4), we arrive at the phenomenological diffusion equation (also known as Fick's second law or the heat equation)

$$\partial_t u(x,t) = Du_{xx}(x,t).$$

$J(x,t)$ denotes the flux of the diffusivity component, where flux is defined as the net movement of the diffusing material per unit area. $u(x,t)$ denotes the concentration or temperature of the diffusing material and D is the diffusivity constant. D depends on the diffusing material and the medium it is diffusing through.

As mentioned earlier, the phenomenological diffusion equation is a parabolic partial differential equation and models the non-physical property of infinite speeds of propagation.

2.2 The Cattaneo equation

In 1948 Cattaneo replaced the constitutive equation (2.1) by

$$J(x,t) + \tau\partial_t J(x,t) = -Du_x(x,t). \tag{2.5}$$

This relaxes the flux.

Differentiating (2.5) with respect to x

$$J_x(x,t) + \tau \partial_t J_x(x,t) = -D u_{xx}(x,t) \tag{2.6}$$
$$\Rightarrow J_x(x,t) = \frac{-D u_{xx}(x,t)}{(1+\tau\partial_t)}.$$

Now substitute (2.6) into the mass balance equation (2.2) to obtain Cattaneo's equation

$$\begin{aligned} \partial_t u(x,t) &= \frac{D u_{xx}(x,t)}{(1+\tau\partial_t)} \\ \Rightarrow \partial_t u(x,t) + \tau \partial_t^2 u(x,t) &= D u_{xx}(x,t). \end{aligned}$$

We note that, by extending the phenomenological diffusion equation through the use of (2.11), the problem of infinite propagation is overcome. The Cattaneo equation is a generalisation of the heat diffusion and particle diffusion equations. However, the MSD (mean-square displacement) is not manifested by the Cattaneo equation as is the case for anomalous diffusion. This is the reason why Compte and Metzler [12] investigated generalisations of the Cattaneo equation.

2.3 The generalised Cattaneo equation I

An introduction of a fractional derivative (to add memory to the equation) and an *ad hoc* generalisation of the continuity equation (2.2) relaxes the flux to give

$$\partial_t^{\gamma} u(x,t) = -J_x(x,t). \tag{2.7}$$

Combining (2.7) with the modified constitutive equation (1.12) yields the first generalised Cattaneo equation (1.13). Differentiating equa-

tion (1.12) with respect to x we obtain

$$J_x(x,t) + \tau^\gamma \partial_t^\gamma J_x(x,t) = -D u_{xx}(x,t) \tag{2.8}$$
$$\Rightarrow J_x(x,t) = \frac{-D u_{xx}(x,t)}{(1+\tau^\gamma \partial_t^\gamma)}.$$

Combining equation (2.8) with the generalised continuity equation (2.7) we obtain GCE I (1.13)

$$\begin{aligned} \partial_t^\gamma u(x,t) &= \frac{D u_{xx}(x,t)}{(1+\tau^\gamma \partial_t^\gamma)} \\ \Rightarrow \partial_t^\gamma u(x,t) + \tau^\gamma \partial_t^{2\gamma} u(x,t) &= D u_{xx}(x,t). \qquad \text{(GCE I)} \end{aligned}$$

Since there is an introduction of fractional derivatives based on stochastic continuous time random walks, $u(x,t)$ is redefined as the probability distribution function of the diffusing material. It represents the probability or predicts the likelihood of finding a particle being at a position x at a time t.

There is an alternate way of reaching GCE I that Compte and Metzler [12] mention through the combination of the mass balance equation (2.2) and the modified constitutive equation

$$J(x,t) + \tau^\gamma \partial_t^\gamma J_x(x,t) = -D \partial_t^{1-\gamma} u_x(x,t). \tag{2.9}$$

We differentiate this equation with respect to x

$$J_x(x,t) + \tau^\gamma \partial_t^\gamma J_x(x,t) = -D \partial_t^{1-\gamma} u_{xx}(x,t) \tag{2.10}$$
$$\Rightarrow J_x(x,t) = \frac{-D \partial_t^{1-\gamma} u_{xx}(x,t)}{(1+\tau^\gamma \partial_t^\gamma)}.$$

Substituting equation (2.10) into the mass balance equation (2.2) and applying the property of fractional derivatives $\partial_t^\alpha \partial_t^\beta = \partial_t^{\alpha+\beta}$

[12, 37] will yield GCE I

$$\begin{aligned}
\partial_t u(x,t) &= \frac{D\partial_t^{1-\gamma} u_{xx}(x,t)}{(1+\tau^\gamma \partial_t^\gamma)} \\
\Rightarrow \partial_t^{\gamma-1}\partial_t u(x,t) + \tau^\gamma \partial_t^\gamma \partial_t^{\gamma-1}\partial_t u(x,t) &= D u_{xx}(x,t) \\
\Rightarrow \partial_t^\gamma u(x,t) + \tau^\gamma \partial_t^{2\gamma} u(x,t) &= D u_{xx}(x,t). \qquad \text{(GCE I)}
\end{aligned}$$

2.4 The generalised Cattaneo equation II

Another form of the modified constitutive equation is used for the second generalisation

$$J(x,t) + \tau^\gamma \partial_t^\gamma J(x,t) = -D\partial_t^{\gamma-1} u_x(x,t). \tag{2.11}$$

Differentiating (2.11) with respect to x

$$\begin{aligned}
J_x(x,t) + \tau^\gamma \partial_t^\gamma J_x(x,t) &= -D\partial_t^{\gamma-1} u_{xx}(x,t) \qquad (2.12) \\
\Rightarrow J_x(x,t) &= \frac{-D\partial_t^{\gamma-1} u_{xx}(x,t)}{(1+\tau^\gamma \partial_t^\gamma)}.
\end{aligned}$$

Substitute (2.12) into the mass balance equation (2.2) and again making use of the property of fractional derivatives as mentioned for the derivation of GCE I we obtain GCE II (1.15)

$$\begin{aligned}
\partial_t u(x,t) &= \frac{D\partial_t^{\gamma-1} u_{xx}(x,t)}{(1+\tau^\gamma \partial_t^\gamma)} \\
\Rightarrow \partial_t^{1-\gamma}\partial_t u(x,t) + \tau^\gamma \partial_t \partial_t u(x,t) &= D u_{xx}(x,t) \\
\Rightarrow \partial_t^{2-\gamma} u(x,t) + \tau^\gamma \partial_t^2 u(x,t) &= D u_{xx}(x,t). \qquad \text{(GCE II)}
\end{aligned}$$

2.5 The generalised Cattaneo equation III

The combination of the *ad hoc* generalised continuity equation given by (2.7) with Cattaneo's replaced equation (1.9) will yield the third generalised Cattaneo equation (1.16). Differentiate equation (2.11) with respect to x to obtain

$$\begin{aligned} J_x(x,t) + \tau \partial_t J_x(x,t) &= -D u_{xx}(x,t) \\ \Rightarrow J_x(x,t) &= \frac{-D u_{xx}(x,t)}{(1+\tau\partial_t)}, \end{aligned}$$

which can be substituted into (2.7) to get GCE III (1.16)

$$\begin{aligned} \partial_t^\gamma u(x,t) &= \frac{D u_{xx}(x,t)}{(1+\tau\partial_t)} \\ \Rightarrow \partial_t^\gamma u(x,t) + \tau \partial_t \partial_t^\gamma u(x,t) &= D u_{xx}(x,t) \\ \Rightarrow \partial_t^\gamma u(x,t) + \tau \partial_t^{1+\gamma} u(x,t) &= D u_{xx}(x,t). \qquad \text{(GCE III)} \end{aligned}$$

Compte and Metzler [12] investigate the properties of the generalised Cattaneo equations by recovering the corresponding MSD and phase velocity equations. It is concluded that GCE I and GCE III show an infinite propagation, as in standard Fickian diffusion. GCE II is shown to describe pure ballistic transport and displays a finite velocity of propagation. GCE I and GCE III models subdiffusion, while GCE II models superdiffusion.

The explanation of these properties originates from their derivations. The derivation of GCE II is associated with long-tail waiting times and is time reversible for sufficiently small times. GCE I and

GCE III seem similar, however, the τ appearing in GCE I is associated with the waiting time distribution of fractal time random walks. In GCE III, τ is just the delay time that was introduced in the constitutive equation (1.9).

Compte and Metzler [12] use a standard Fourier-Laplace transform technique to obtain (x,t)-space equations for each GCE. The observation is made from these that the solutions to the GCE's lead to a modified Gaussian behaviour.

2.6 Numerical schemes through discretization

We define the integration time as $t_j = j\Delta t$ where $0 \leq t_j \leq T$, T being the termination time or the final time to which we run the numerical scheme. We define the spatial grid size as $\Delta x = \dfrac{x_R - x_L}{n}$, with $x_i = x_L + i\Delta x$ for $i = 0, \ldots, n$; n is a positive integer ($(n+1)$ is the number of spatial points) and each grid point lies in the interval $x_L < x_i < x_R$. We use the notation u_i^j as the numerical approximation of u at (x_i, t_j).

Finite difference methods are used to discretize our equations. Finite difference formulae for derivatives are derived using a Taylor series expansion. It is well known that the Taylor series expansion of a function about a given point includes all higher order terms.

Normally most of these higher order terms are neglected [13] as the error presented is negligible [41]. These errors terms are known as the local truncation error. The difference methods are calculated such that their local truncation errors are $O(h^p)$, with a high value of p as possible [41] where $h << 1$ (i.e. if $h << 1$, where h is the step-length, then $O(h^p)$ and error is very small). This explains why the numerical solutions obtained (which are always stated to a finite number of figures) introduce round off errors.

For our scheme we consider the diffusion of point sources for $u(x, 0) = \delta(x)$, where $\delta(x)$ is defined as the Dirac delta function, and the boundary condition $u(\pm\infty, t) = 0$.

We approximate the Dirac delta function by

$$\delta(x) = \frac{1}{\eta\sqrt{\pi}} \exp\left(\frac{-x^2}{\eta^2}\right), \tag{2.13}$$

where η is a constant and we choose $\eta = 1$.
The analogy used in the introductory chapter of heat diffusion through a rod represents a system that is acted upon by an external force of large magnitude but that acts for a short period of time. The Dirac delta function is a type of unit impulse that serves as a mathematical model for such a force [14].

Since we are discretizing each equation to have a spatial grid of finite size n, applying the boundary condition as defined implies $u_0^j = 0$ and $u_n^j = 0$ for all j. The boundary conditions for the physical

problem are specified at infinity. For the computational application we make the boundaries finite. We choose $u(-10,t) = u(10,t) = 0$ or $u(-20,t) = u(20,t) = 0$ or $u(-30,t) = u(30,t) = 0$ depending on the equation we are solving.

Crank [13] describes a point source as "a single, identifiable localised source of something and is approximated as a mathematical point to simplify analysis". When a change is introduced to a system, as described by anomalous diffusion, we are delivering an impulse to the system. If the source of change is at any point in the system (other than a point of origin x_0,), for example at $x = s$, then the response of the system to the change shifts by an amount of s. No matter where an impulse is delivered to the system, the impulse will diffuse through and we can draw equivalent conclusions about the particles of the system. Another way to think of it is that any point in the system can be a source point. Thus, every $u(x_i, 0)$ is an integral of point sources, the integral is $\int \delta(x-s)u(s-0)ds$ [13].

Thus at any point in the system, we can introduce an impulse of dissipating energy through the system. This allows us to observe how an impulse diffuses through a system and how the particles are likely to respond to it. The Dirac delta function is useful for approximating an impulse which is used to simplify equations and calculations.

We compare solutions of the fractional diffusion equation and the

fractional Cattaneo equation. We consider both fractional time and spatial derivatives. The values for D, α and β are chosen across the respective intervals ($0 < \alpha < 1$, $1 < \beta \leq 2$) to investigate the solutions for a range of different values chosen. For the case of this study $\Delta x = 0.1$ and $\Delta t = 0.01$.

3 Fractional diffusion equations

In this chapter we derive numerical schemes to determine approximate numerical solutions to fractional diffusion equations.

We consider a fractional time diffusion equation, where the fractional derivative operates on time. Then we consider a fractional diffusion equation where the fractional derivative operates on space.

3.1 Fractional time diffusion equation

Consider the time α-order fractional partial differential equation

$$\frac{\partial^\alpha u}{\partial t^\alpha} = D\frac{\partial^2 u}{\partial x^2}, \tag{3.1}$$

where $0 < \alpha < 1$ and D is the diffusion constant.

If $\alpha = 1$ the phenomenological diffusion equation (1.7) is recovered.
The point source solution of the phenomenological diffusion equation, which is typically Gaussian, is

$$u(x,t) = \frac{1}{(4\pi Dt)^{\frac{1}{2}}} \exp\left(-\frac{x^2}{4Dt}\right). \tag{3.2}$$

We refer to the technique described by Yuste and Acedo [48] where the fractional time derivative is approximated by the Grünwald-Letnikov definition; we choose $h = \Delta t$

$$ {}_0D_t^{1-\alpha} u = \frac{\partial^{1-\alpha} u}{\partial t^{1-\alpha}} = \lim_{h \to 0} \frac{1}{h^{(1-\alpha)}} \sum_{k=0}^{n} w_k^{(1-\alpha)} u(x, t - kh), \tag{3.3} $$

where the weights are defined as

$$ w_k^{(\gamma)} = (-1)^k \binom{\gamma}{k}. $$

The following property of fractional calculus [12, 37]

$$ \frac{\partial^\alpha}{\partial t^\alpha} \frac{\partial^\beta}{\partial t^\beta} = \frac{\partial^{\alpha+\beta}}{\partial t^{\alpha+\beta}}, $$

allows us to multiply equation (3.1) by the operator $\dfrac{\partial^{1-\alpha}}{\partial t^{1-\alpha}}$ to obtain the following equation

$$ \frac{\partial u}{\partial t} = D \left({}_0D_t^{1-\alpha} \frac{\partial^2 u}{\partial x^2} \right). $$

A forward difference approximation is applied to the $\dfrac{\partial u}{\partial t}$ term and a central difference approximation is used to discretize the $\dfrac{\partial^2 u}{\partial x^2}$ term to obtain the equation

$$ \frac{u_i^{j+1} - u_i^j}{\Delta t} = \frac{D}{\Delta x^2} \quad {}_0D_t^{1-\alpha} (u_{i+1}^j - 2u_i^j + u_{i-1}^j). $$

Employing the Grünwald-Letnikov definition and rearranging we obtain the following scheme

$$ u_i^{j+1} = u_i^j + \lambda \sum_{k=0}^{j} w_k^{(1-\alpha)} (u_{i+1}^{j-k} - 2u_i^{j-k} + u_{i-1}^{j-k}), \tag{3.4} $$

where, for convenience, $\lambda = \dfrac{D(\Delta t)^{\alpha}}{(\Delta x)^2}$.
Note that we require values for u at the spatial points x_{-1} and x_{n+1} which lie outside of the interval of collocation points $x_0 \leq x_i \leq x_n$. Since we have defined the boundary condition as $u(\pm\infty, t) = 0$, this allows us to make the replacements: $u_1^j = u_{-1}^j$ and $u_{n+1}^j = u_{n-1}^j$.

We can start this scheme from $j = 0$ to calculate a value for u at the next time-step $j = 1$. If $j = 1$, the scheme then calculates a value for u at $j = 2$; and so on until we obtain a numerical solution for u at the predefined final time T ($j = n-1$ to calculate $u(x_i, t_n)$).

Writing this out line by line, we obtain the following explicit scheme:

$$
\begin{aligned}
\text{For} \quad j &= 0: \\
u_i^1 &= u_i^0 + \lambda w_0^{(1-\alpha)}(u_{i+1}^0 - 2u_i^0 + u_{i-1}^0) \\
\text{For} \quad j &= 1: \\
u_i^2 &= u_i^1 + \lambda \left(w_0^{(1-\alpha)}(u_{i+1}^1 - 2u_i^1 + u_{i-1}^1) + w_1^{(1-\alpha)}(u_{i+1}^0 - 2u_i^0 + u_{i-1}^0) \right)
\end{aligned}
$$

For $j = 2$:

$$
\begin{aligned}
u_i^3 = u_i^2 + \lambda(w_0^{(1-\alpha)}(u_{i+1}^2 - 2u_i^2 + u_{i-1}^2) + w_1^{(1-\alpha)}(u_{i+1}^1 - 2u_i^1 + u_{i-1}^1) \\
+ w_2^{(1-\alpha)}(u_{i+1}^0 - 2u_i^0 + u_{i-1}^0))
\end{aligned}
$$

$\vdots$

$\vdots$

$\vdots$

For $j = n-2$:

$$u_i^{n-1} = u_i^{n-2} + \lambda(w_0^{(1-\alpha)}(u_{i+1}^{n-2} - 2u_i^{n-2} + u_{i-1}^{n-2}) + w_1^{(1-\alpha)}(u_{i+1}^{n-3} - 2u_i^{n-3} + u_{i-1}^{n-3}) + \cdots + w_{n-2}^{(1-\alpha)}(u_{i+1}^{0} - 2u_i^{0} + u_{i-1}^{0}))$$

For $j = n-1$:

$$u_i^{n} = u_i^{n-1} + \lambda(w_0^{(1-\alpha)}(u_{i+1}^{n-1} - 2u_i^{n-1} + u_{i-1}^{n-1}) + w_1^{(1-\alpha)}(u_{i+1}^{n-2} - 2u_i^{n-2} + u_{i-1}^{n-2}) + \cdots + w_{n-1}^{(1-\alpha)}(u_{i+1}^{0} - 2u_i^{0} + u_{i-1}^{0})).$$

If, for each collocation point x_i $(i = 1, \ldots, n)$ we fix the time-step t_j and examine the explicit system we see that for each new time-step t_{j+1} the value $u(x_i, t_{j+1})$ depends on all the $u(x_i, t_j)$ values calculated at all the previous time-steps. This represents the memory effect mentioned earlier.

We use Mathematica to create a matrix where the first column represents the initial condition applied to each x_i collocation point. The rest of the columns represent the next time-step $j+1$ for u_i and are calculated using the scheme (3.4). We find numerical solutions for different values of the diffusion coefficient $D = 0.1, 0.5, 1, 1.5$. For each value of D we adjust the value of α as follows: $\alpha = 0.1, 0.5, 0.9$. We then plot the solutions found at $t = 0, 0.1, 0.5, 1$. The chosen interval is $[-30, 30]$ as this is large enough to satisfy the boundary conditions. When running the scheme for larger values of t, it becomes more memory intensive (caused by the memory effect explained earlier) and takes longer to run, though still with converging results.

When numerical solutions are plotted for $\alpha = 0.1$, $\alpha = 0.5$ and

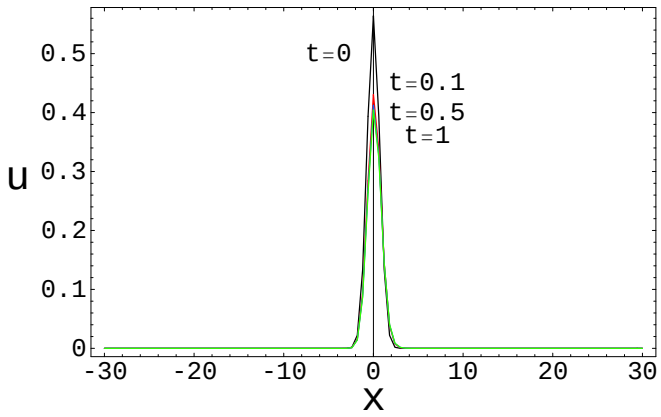

Figure 4: Numerical solutions for fractional time diffusion equation (3.1) at times $t = 0$ (black), $t = 0.1$ (red), $t = 0.5$ (blue) and $t = 1$ (green), where $\alpha = 0.1$ and $D = 0.1$. Diffusive behaviour is observed very slightly when final time is 1.

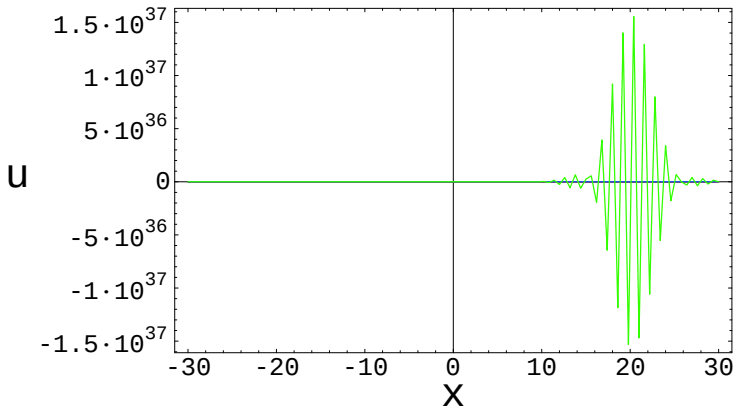

Figure 5: Numerical solutions for fractional time diffusion equation (3.1) where $\alpha = 0.1$ and $D = 0.5$, showing oscillatory behaviour.

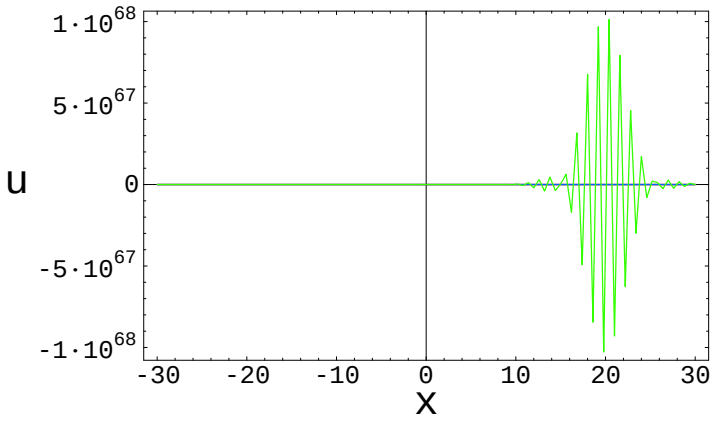

Figure 6: Numerical solutions for fractional time diffusion equation (3.1) where $\alpha = 0.1$ and $D = 1$, showing oscillatory behaviour.

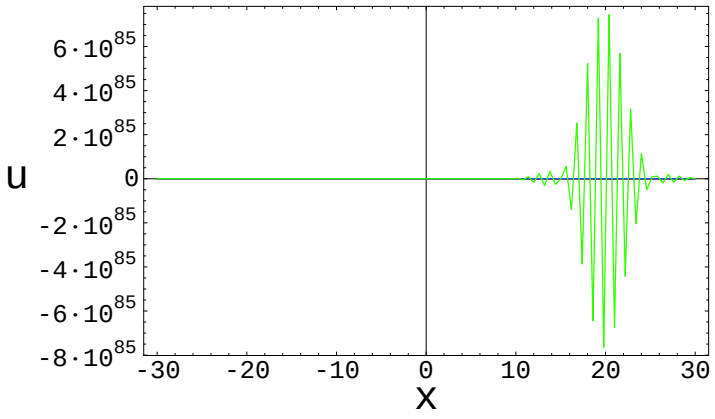

Figure 7: Numerical solutions for fractional time diffusion equation (3.1) where $\alpha = 0.1$ and $D = 1.5$, showing oscillatory behaviour.

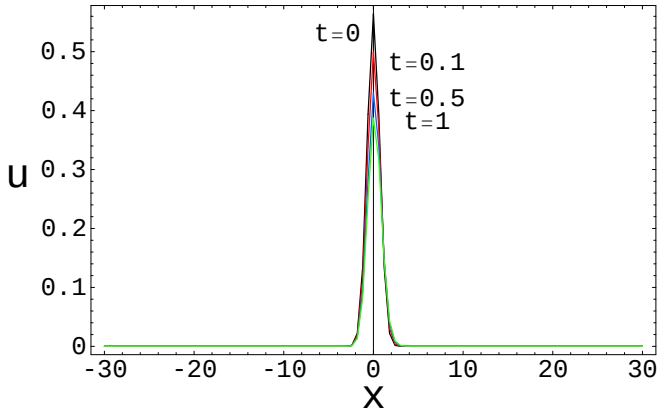

Figure 8: Numerical solutions for fractional time diffusion equation (3.1) where $\alpha = 0.5$ and $D = 0.1$, from $t = 0$ (black), $t = 0.1$ (red), $t = 0.5$ (blue), until $t = 1$ (green). Solution shows that diffusion occurs very slowly over time.

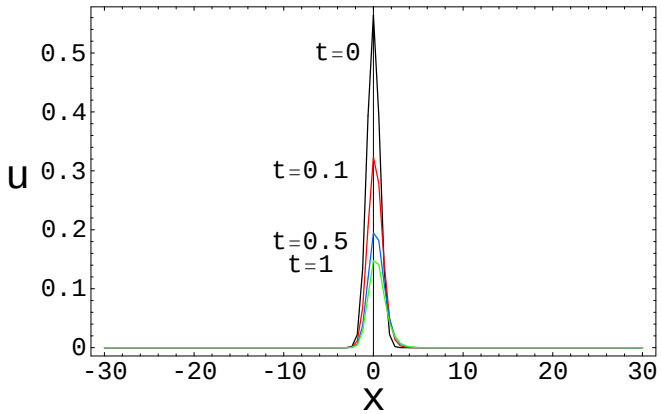

Figure 9: Numerical solutions for fractional time diffusion equation (3.1) where $\alpha = 0.5$ and $D = 0.5$. Solution had been been plotted for times $t = 0$ (black), $t = 0.1$ (red), $t = 0.5$ (blue) and $t = 1$ (green). Diffusion occurs more visibly than for $D = 0.1$ (Figure 8).

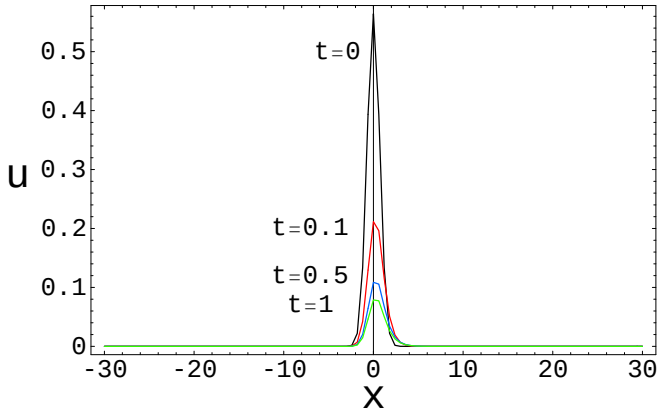

Figure 10: Numerical solutions for fractional time diffusion equation (3.1) where $\alpha = 0.5$ and $D = 1$. Superdiffusion is observed over time ($t = 0$ (black), $t = 0.1$ (red), $t = 0.5$ (blue) and $t = 1$ (green)).

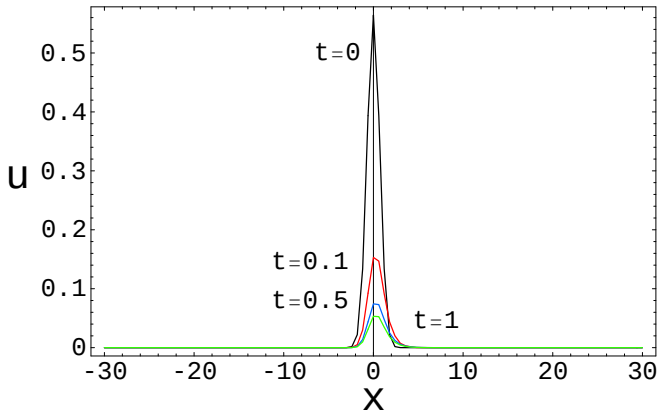

Figure 11: Numerical solutions for fractional time diffusion equation (3.1) where $\alpha = 0.5$ and $D = 1.5$. Superdiffusion is observed, but at a faster pace than when $D = 1$ (Figure 10). Times results are plotted at are $t = 0$ (black), $t = 0.1$ (red), $t = 0.5$ (blue) and $t = 1$ (green).

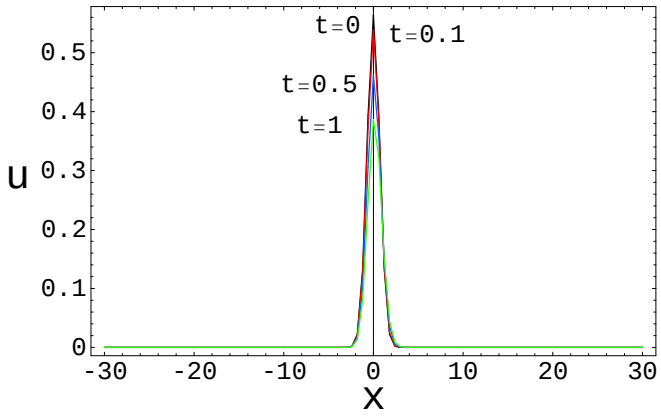

Figure 12: Numerical solutions for fractional time diffusion equation (3.1) where $\alpha = 0.9$ and $D = 0.1$. The diffusion process appears to have taken place, but very slowly. Times results are plotted at are $t = 0$ (black), $t = 0.1$ (red), $t = 0.5$ (blue) and $t = 1$ (green).

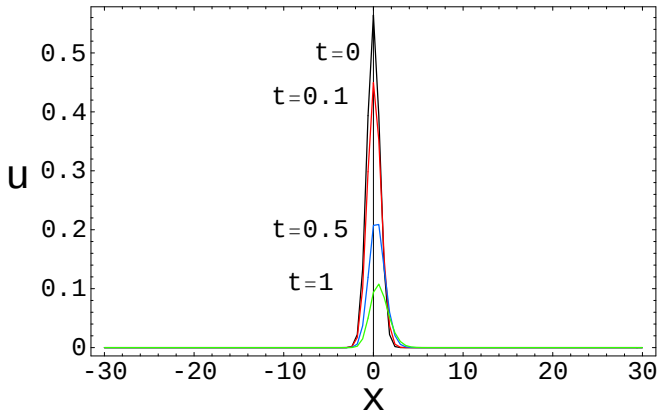

Figure 13: Numerical solutions for fractional time diffusion equation (3.1) where $\alpha = 0.9$ and $D = 0.5$. Diffusion occurs more rapidly and superdiffusion is observed as final time $t = 1$ (green) is approached. Times results are plotted at are $t = 0$ (black), $t = 0.1$ (red), $t = 0.5$ (blue) and $t = 1$ (green).

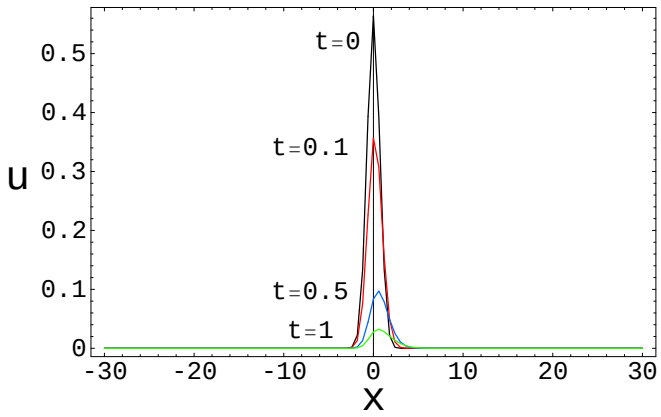

Figure 14: Numerical solutions for fractional time diffusion equation (3.1) where $\alpha = 0.9$ and $D = 1$ over time $t = 0$ (black), $t = 0.1$ (red), $t = 0.5$ (blue) and $t = 1$ (green). Superdiffusion is observed.

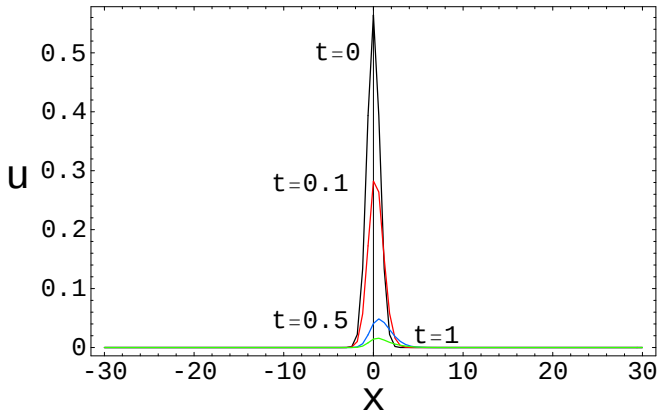

Figure 15: Numerical solutions for fractional time diffusion equation (3.1) where $\alpha = 0.9$ and $D = 1.5$. Over times $t = 0$ (black), $t = 0.1$ (red), $t = 0.5$ (blue) and $t = 1$ (green) superdiffusion is observed.

$\alpha = 0.9$ with $D = 0.1$, diffusive behaviour is observed to only just start taking place as shown by Figures 4, 8, 12. However when D is changed to $0.5, 1$ and 1.5 the solution oscillates for times $t = 0.1, 0.5, 1$ (Figures 5, 6, 7). As we increase the value of D for each value of α, diffusion occurs much quicker and is more visible (Figures 9, 10, 13, 14). Figure 11 shows diffusion is much faster than for a smaller α in Figure 15.

3.2 Fractional space diffusion equation

Consider the space β-order fractional partial differential equation

$$\frac{\partial u}{\partial t} = D\frac{\partial^\beta u}{\partial x^\beta} \tag{3.5}$$

where $1 < \beta \leq 2$ and D is the diffusion coefficient.

For a fractional space derivative we refer to the technique described by Tadjeran *et al* [7]. Here the fractional space derivative is approximated by the right-shifted Grünwald definition and a Crank-Nicholson average over time.

The right-shifted Grünwald formula is given as

$$\frac{\partial^\beta u(x,t)}{\partial x^\beta} = \lim_{n\to\infty} \frac{1}{(\Delta x)^\beta} \sum_{k=0}^{n} g_{\beta,k} u(x-(k-1)h, t) \tag{3.6}$$

where

$$g_{\beta,k} = \frac{\Gamma(k-\beta)}{\Gamma(-\beta)\Gamma(k+1)}$$

are the normalized Grünwald weights and we choose $h = \Delta x$.

Applying a forward difference approximation to the time derivative and definition (3.6) we have the following scheme

$$\frac{1}{\Delta t}(u_i^{j+1} - u_i^j) = \frac{D}{2(\Delta x)^\beta}\left(\sum_{k=0}^{i+1} g_{\beta,k} u_{i-k+1}^{j+1} + \sum_{k=0}^{i+1} g_{\beta,k} u_{i-k+1}^{j}\right). \quad (3.7)$$

Rearranging (3.7)

$$u_i^{j+1} - D\frac{\Delta t}{2(\Delta x)^\beta}\sum_{k=0}^{i+1} g_{\beta,k} u_{i-k+1}^{j+1} = u_j^i + D\frac{\Delta t}{2(\Delta x)^\beta}\sum_{k=0}^{i+1} g_{\beta,k} u_{i-k+1}^{j}, \quad (3.8)$$

where we let $\lambda = D\dfrac{\Delta t}{2(\Delta x)^\beta}$.

The left-hand side of (3.8) can be expanded and simplified to obtain

$$-\lambda g_{\beta,k} u_{i+1}^{j+1} + (1 - \lambda g_{\beta,k}) u_i^{j+1} - \lambda g_{\beta,k} u_{i-1}^{j+1} - \cdots - \lambda g_{\beta,k} u_0^{j+1}.$$

Similarly the right-hand side of (3.8) can be expanded and simplified to obtain

$$\lambda g_{\beta,k} u_{i+1}^{j} + (1 + \lambda g_{\beta,k}) u_i^{j} + \lambda g_{\beta,k} u_{i-1}^{j} + \cdots + \lambda g_{\beta,k} u_0^{j}.$$

The problem in matrix form becomes

$$L\underline{u}^{j+1} = R\underline{u}^{j}.$$

Applying the boundary condition, the numerical solution can be obtained at the time-step t_{j+1}

$$\underline{u}^{j+1} = L^{-1} R\underline{u}^{j},$$

where

$$L = \begin{pmatrix} 1 & 0 & \dots & \dots & \dots & \dots & 0 \\ -\lambda g_{\beta,2} & (1-\lambda g_{\beta,1}) & -\lambda g_{\beta,0} & 0 & \dots & \dots & 0 \\ -\lambda g_{\beta,3} & -\lambda g_{\beta,2} & (1-\lambda g_{\beta,1}) & -\lambda g_{\beta,0} & 0 & \dots & 0 \\ \vdots & \ddots & \ddots & \vdots & \vdots & \vdots & \vdots \\ \vdots & \vdots & \ddots & \ddots & \vdots & \vdots & \vdots \\ \vdots & \vdots & \vdots & \ddots & \ddots & \vdots & \vdots \\ -\lambda g_{\beta,n} & -\lambda g_{\beta,n-1} & \dots & \dots & -\lambda g_{\beta,2} & (1-\lambda g_{\beta,1}) & -\lambda g_{\beta,0} \\ 0 & 0 & \dots & \dots & \dots & 0 & 1 \end{pmatrix},$$

$$R = \begin{pmatrix} 1 & 0 & \dots & \dots & \dots & \dots & 0 \\ \lambda g_{\beta,2} & (1+\lambda g_{\beta,1}) & \lambda g_{\beta,0} & 0 & \dots & \dots & 0 \\ \lambda g_{\beta,3} & \lambda g_{\beta,2} & (1+\lambda g_{\beta,1}) & \lambda g_{\beta,0} & 0 & \dots & 0 \\ \vdots & \ddots & \ddots & \vdots & \vdots & \vdots & \vdots \\ \vdots & \vdots & \ddots & \ddots & \vdots & \vdots & \vdots \\ \vdots & \vdots & \vdots & \ddots & \ddots & \vdots & \vdots \\ \lambda g_{\beta,n} & \lambda g_{\beta,n-1} & \dots & \dots & \lambda g_{\beta,2} & (1+\lambda g_{\beta,1}) & \lambda g_{\beta,0} \\ 0 & 0 & \dots & \dots & \dots & 0 & 1 \end{pmatrix}$$

and

$$\begin{aligned} \underline{u}^{j+1} &= [u_0^{j+1}, u_1^{j+1}, \dots, u_{n-1}^{j+1}, u_n^{j+1}]^T, \\ \underline{u}^{j} &= [u_0^{j}, u_1^{j}, \dots, u_{n-1}^{j}, u_n^{j}]^T. \end{aligned}$$

We use Mathematica to implement the scheme and plot the solutions for different values of D: $D = 0.1, 0.5, 1, 1.5$ and adjusting

the fractional order for each value of D: $\beta = 1.2, 1.5, 1.9$ at times $t = 0, 5, 10, 20$ and over the interval $[-50, 50]$ to show the behaviour observed.

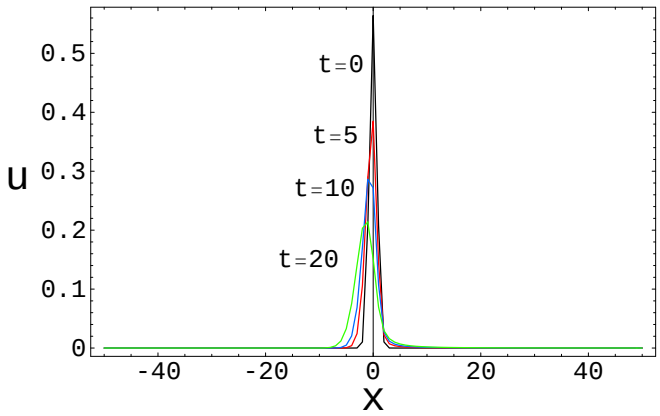

Figure 16: Numerical solutions for fractional space diffusion equation (3.5) at times $t = 0$ (black), $t = 0.1$ (red), $t = 0.5$ (blue) and $t = 1$ (green); where $\beta = 1.2$ and $D = 0.1$. Normal diffusion is displayed.

If we refer to Figures 16 through to 27 and observe the results obtained from $D = 0.1$, $D = 0.5$, $D = 1$ and $D = 1.5$ for each β we chose, it is shown that with a higher value of D, diffusion occurs much faster. When β is 1.2 and 1.5, results are distributed skewed to the left, behaviour relating to the right-shifted Grünwald formula. However, for a higher value of β, $\beta = 1.9$, the results (Figures 24, 25, 26, 27) show a more Gaussian behaviour, with a normal distribution.

In this chapter we have considered numerical solutions of the frac-

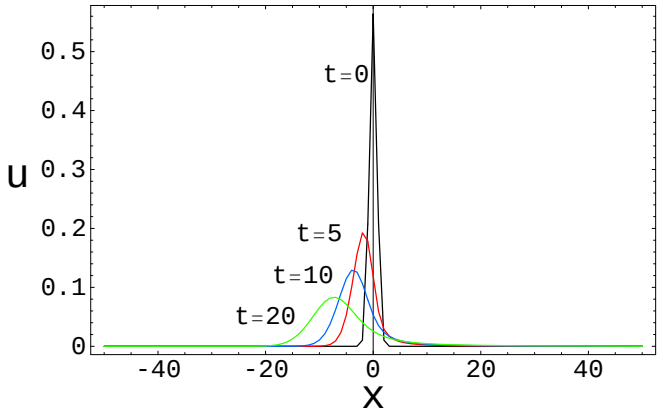

Figure 17: Numerical solutions for fractional space diffusion equation (3.5) where $\beta = 1.2$ and $D = 0.5$ for times $t = 0$ (black), $t = 0.1$ (red), $t = 0.5$ (blue) and $t = 1$ (green).

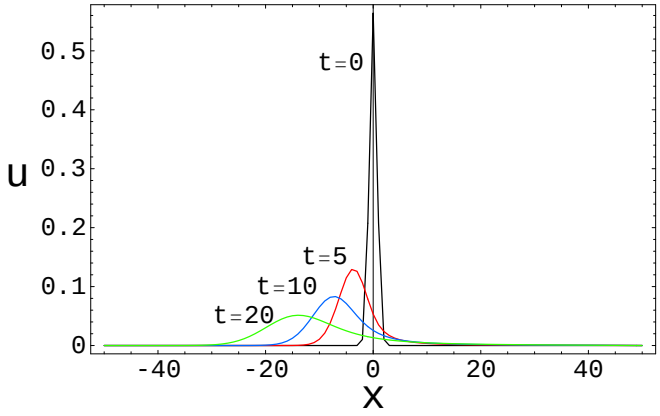

Figure 18: Numerical solutions for fractional space diffusion equation (3.5) where $\beta = 1.2$ and $D = 1$. Results display superdiffusion, being skewed to the left over times $t = 0$ (black), $t = 0.1$ (red), $t = 0.5$ (blue) and $t = 1$ (green).

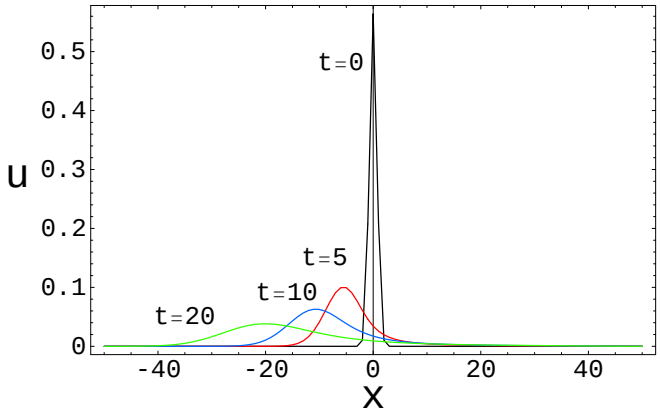

Figure 19: Numerical solutions for fractional space diffusion equation (3.5) where $\beta = 1.2$ and $D = 1.5$. Diffusion occurs faster compared to when $D = 1$ for times $t = 0$ (black), $t = 0.1$ (red), $t = 0.5$ (blue) and $t = 1$ (green).

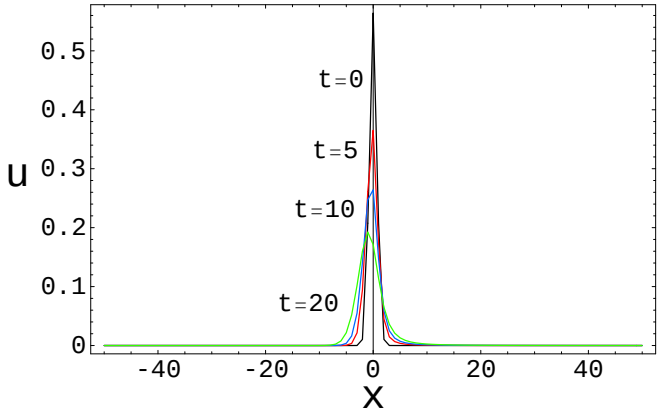

Figure 20: Numerical solutions for fractional space diffusion (3.5) equation where $\beta = 1.5$ and $D = 0.1$. Normal diffusion behaviour is observed over times $t = 0$ (black), $t = 0.1$ (red), $t = 0.5$ (blue) and $t = 1$ (green).

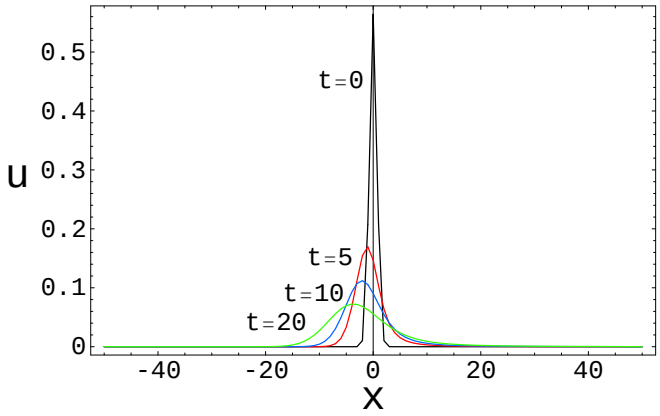

Figure 21: Numerical solutions for fractional space diffusion (3.5) equation where $\beta = 1.5$ and $D = 0.5$. Results display a faster diffusion process occurring compared to $\beta = 1.2$ ($t = 0$ (black), $t = 0.1$ (red), $t = 0.5$ (blue) and $t = 1$ (green)).

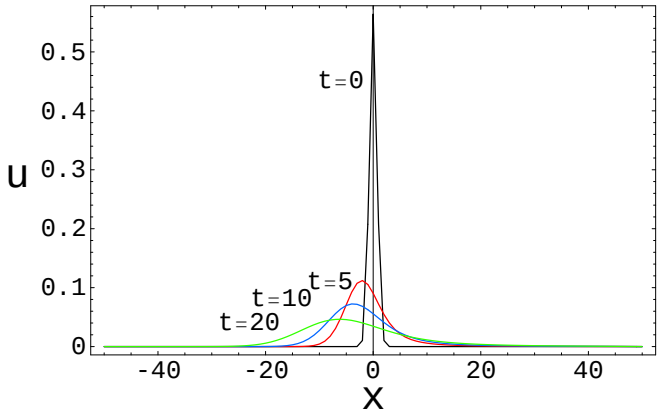

Figure 22: Numerical solutions for fractional space diffusion equation (3.5) for $t = 0$ (black), $t = 0.1$ (red), $t = 0.5$ (blue) and $t = 1$ (green), where $\beta = 1.5$ and $D = 1$. Diffusion appears to take place faster with increasing D.

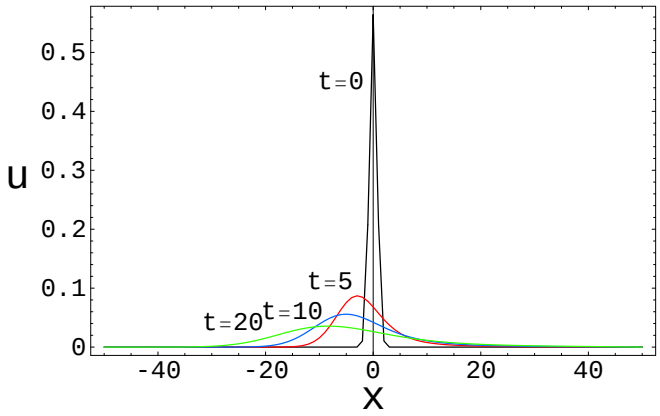

Figure 23: Numerical solutions for fractional space diffusion equation (3.5) for $t = 0$ (black), $t = 0.1$ (red), $t = 0.5$ (blue) and $t = 1$ (green), where $\beta = 1.5$ and $D = 1.5$. Diffusion appears to take place faster with increasing D.

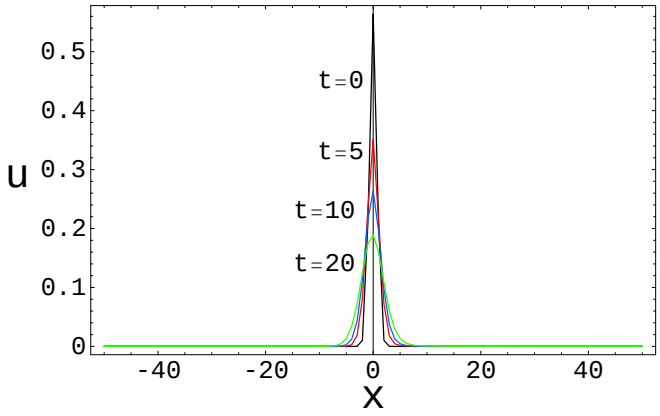

Figure 24: Numerical solutions for fractional space diffusion equation (3.5) for $t = 0$ (black), $t = 0.1$ (red), $t = 0.5$ (blue) and $t = 1$ (green), where $\beta = 1.9$ and $D = 0.1$. Diffusion takes place faster with a normal distribution when compared to other values of β when $D = 0.1$.

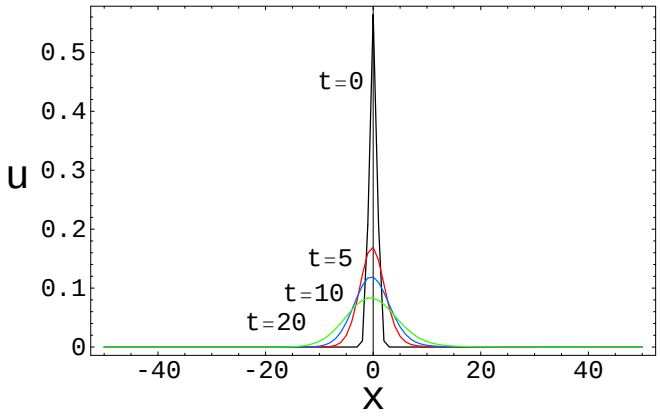

Figure 25: Numerical solutions for fractional space diffusion equation (3.5) for $t = 0$ (black), $t = 0.1$ (red), $t = 0.5$ (blue) and $t = 1$ (green), where $\beta = 1.9$ and $D = 0.5$. Superdiffusion is observed with a normal distribution.

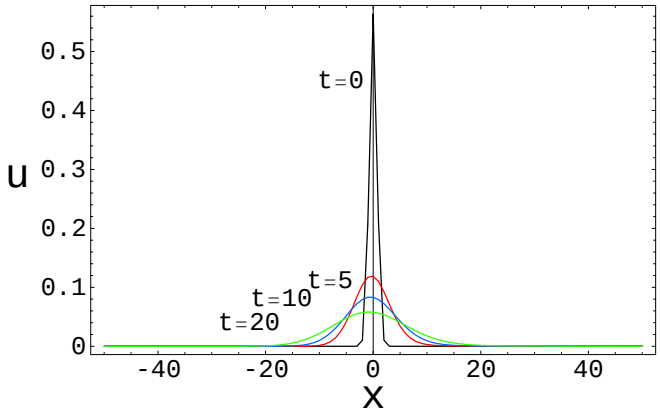

Figure 26: Numerical solutions for fractional space diffusion equation (3.5) for $t = 0$ (black), $t = 0.1$ (red), $t = 0.5$ (blue) and $t = 1$ (green), where $\beta = 1.9$ and $D = 1$. Superdiffusion is observed with a normal distribution.

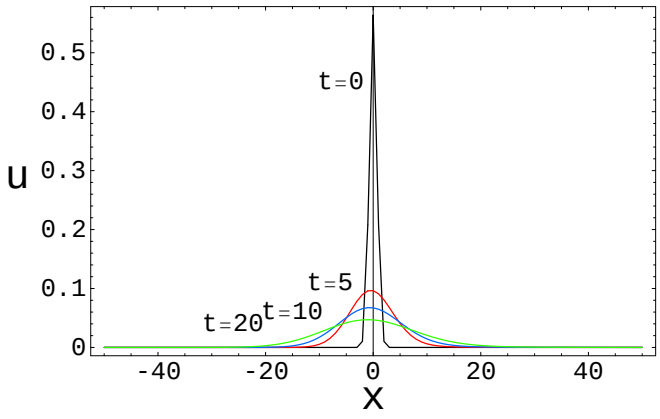

Figure 27: Numerical solutions for fractional space diffusion equation (3.5) for $t = 0$ (black), $t = 0.1$ (red), $t = 0.5$ (blue) and $t = 1$ (green), where $\beta = 1.9$ and $D = 1.5$. Superdiffusion is observed with a normal distribution, faster than with $D = 1$.

tional time diffusion and fractional space diffusion equations. Numerical results for $D = 0.5, 1, 1.5$ when $\alpha = 0.1$ are unstable and oscillatory behaviour is observed. The stable numerical results display very slight propagation when the fractional derivative operates on the time dimension. Since $\dfrac{\partial^\alpha}{\partial x^\alpha}$ mirrors a power-law step length distribution, it is expected to have results showing properties of propagation for the fractional space diffusion equation.

4 Fractional Cattaneo equations

In the previous chapter we found schemes and approximate numerical solutions to fractional diffusion equations. In this chapter we do the same for fractional Cattaneo equations, where we first consider the fractional derivative operating on time. Thereafter we consider the fractional derivative operating on space.

4.1 Fractional time Cattaneo equation

Consider the following fractional time Cattaneo equation with $0 < \alpha < 1$

$$\frac{\partial^\alpha u}{\partial t^\alpha} = D\frac{\partial^2 u}{\partial x^2} - \tau\frac{\partial^\alpha}{\partial t^\alpha}\left(\frac{\partial u}{\partial t}\right). \tag{4.1}$$

The diffusivity constant is D and $\tau \ll 1$.

If $\alpha = 1$ we recover the normal Cattaneo equation (1.10). The approximate solution for equation (1.10) is [18, 19]

$$u(x,t) = \frac{1}{\sqrt{4\pi t}}\left[1 + \tau\left(\frac{3}{4t} - \frac{x^4}{16t^3}\right)\right]\exp\left(-\frac{x^2}{4t}\right). \tag{4.2}$$

We make use of the same technique used for the fractional time diffusion equation (3.4). We apply the Grünwald-Letnikov definition for the time-fractional derivative; forward difference approximations to discretize the integer-order time derivative and a central difference approximations to discretize the second order spatial and time derivatives. We take this approach after multiplying equation

(4.1) by the operator $\frac{\partial^{1-\alpha}}{\partial t^{1-\alpha}}$,as was done for the fractional time diffusion equation in Chapter 3.1. Thus, the system to discretize is

$$\frac{\partial u}{\partial t} = D \quad {}_0D_t^{1-\alpha}\frac{\partial^2 u}{\partial x^2} - \tau\frac{\partial^2 u}{\partial t^2}.$$

The discretized scheme then obtained is given by

$$u_i^{j+1} = c_1 u_i^j - c_2 u_i^{j-1} + c_3 \sum_{k=0}^{j} w_k^{1-\alpha}(u_{i+1}^{j-k} - 2u_i^{j-k} + u_{i-1}^{j-k}), \quad (4.3)$$

where we define the following $c_1 = \frac{1+2\delta}{1+\delta}$, $c_2 = \frac{\delta}{1+\delta}$, $c_3 = \frac{\lambda}{1+\delta}$, $\delta = \frac{\tau}{\Delta t}$ and $\lambda = \frac{D\Delta t^\alpha}{\Delta x^2}$. We employ the boundary conditions: $u_1^j = u_{-1}^j$ and $u_{n+1}^j = u_{n-1}^j$.

We follow the same approach as in Chapter 4.1, and note that for each new time-step t_{j+1} the value $u(x_i, t_{j+1})$ depends on all the $u(x_i, t_j)$ values calculated at all the previous time-steps.

Writing out the equation (4.3) line by line, the system is

$$\begin{aligned}
\text{For} \quad j &= 0: \\
u_i^1 &= c_1 u_i^0 + c_3 w_0^{(1-\alpha)}(u_{i+1}^0 - 2u_i^0 + u_{i-1}^0) \\
\text{For} \quad j &= 1: \\
u_i^2 &= c_1 u_i^1 - c_2 u_i^0 + c_3 \left(w_0^{(1-\alpha)}(u_{i+1}^1 - 2u_i^1 + u_{i-1}^1) + w_1^{(1-\alpha)}(u_{i+1}^0 - 2u_i^0 + u_{i-1}^0) \right)
\end{aligned}$$

For $j = 2$:

$$u_i^3 = c_1 u_i^2 - c_2 u_i^1 + c_3(w_0^{(1-\alpha)}(u_{i+1}^2 - 2u_i^2 + u_{i-1}^2) + w_1^{(1-\alpha)}(u_{i+1}^1 - 2u_i^1 + u_{i-1}^1) + w_2^{(1-\alpha)}(u_{i+1}^0 - 2u_i^0 + u_{i-1}^0))$$

$$\vdots$$

$$\vdots$$

$$\vdots$$

For $j = n-2$:

$$u_i^{n-1} = c_1 u_i^{n-2} - c_2 u_i^{n-3} + c_3(w_0^{(1-\alpha)}(u_{i+1}^{n-2} - 2u_i^{n-2} + u_{i-1}^{n-2})$$
$$+w_1^{(1-\alpha)}(u_{i+1}^{n-3} - 2u_i^{n-3} + u_{i-1}^{n-3}) + \cdots + w_{n-2}^{(1-\alpha)}(u_{i+1}^{0} - 2u_i^{0} + u_{i-1}^{0}))$$

For $j = n-1$:

$$u_i^{n} = c_1 u_i^{n-1} - c_2 u_i^{n-2} + c_3(w_0^{(1-\alpha)}(u_{i+1}^{n-1} - 2u_i^{n-1} + u_{i-1}^{n-1})$$
$$+w_1^{(1-\alpha)}(u_{i+1}^{n-2} - 2u_i^{n-2} + u_{i-1}^{n-2}) + \cdots + w_{n-1}^{(1-\alpha)}(u_{i+1}^{0} - 2u_i^{0} + u_{i-1}^{0})).$$

We use Mathematica and the same approach applied previously to solve the fractional time diffusion equation. The scheme is implemented for $D = 0.1, 0.5, 1, 1.5$ and, for each D, $\alpha = 0.1, 0.5, 0.9$. We plot the solutions over the interval $[-10, 10]$, as this is the smallest interval that satisfies the boundary conditions, unless otherwise stated. We note that due to the memory effect when running the scheme for larger values of t, it becomes more memory intensive and takes longer to run, but still converges.

Solutions for $\alpha = 0.1$, $D = 0.1$ and $\alpha = 0.9$, $D = 1$ (Figure 28, 38), have been calculated using $\Delta t = 0.01$ over times $t = 0, 0.1, 0.25, 0.5$. This choice of parameters sufficiently shows diffusive behaviour, with the solution in Figure 38 showing rapid diffusive behaviour. Solutions for $\alpha = 0.5$, $D = 0.1$; $\alpha = 0.5$, $D = 0.5$; $\alpha = 0.9$, $D = 0.1$ and $\alpha = 0.9$, $D = 0.5$ (Figure 32, 33, 36, 37) have been calculated using $\Delta t = 0.01$ over times $t = 0, 0.1, 0.5, 1$ showing diffusive behaviour.

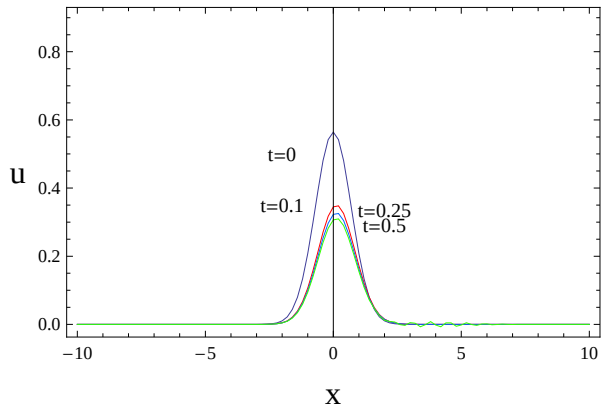

Figure 28: Numerical solutions for fractional time Cattaneo equation (4.1) where $\alpha = 0.1$ and $D = 0.1$. Diffusion occurs overt the times $t = 0.1$ (red), $t = 0.25$ (blue) and $t = 0.5$ (green).

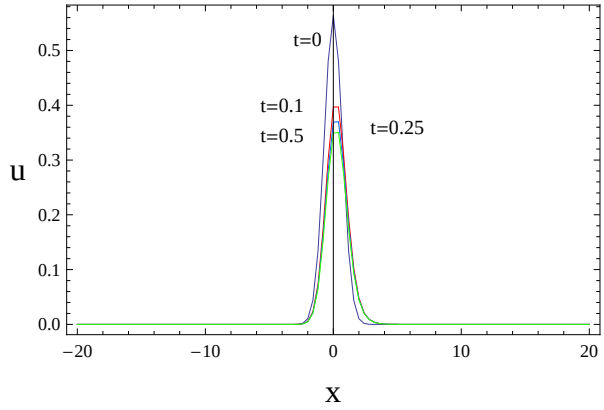

Figure 29: Numerical solutions for fractional time Cattaneo equation (4.1) for $t = 0$ (black), $t = 0.1$ (red), $t = 0.25$ (blue) and $t = 0.5$ (green), where $\alpha = 0.1$ and $D = 0.5$. The system shows slow diffusive behaviour compared to when $D = 0.1$.

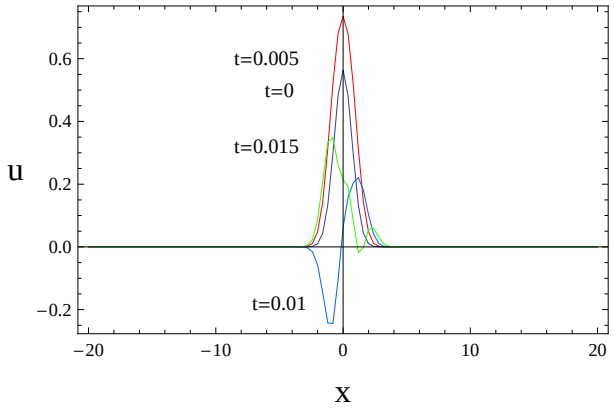

Figure 30: Numerical solutions for fractional time Cattaneo equation (4.1) for $t = 0$ (black), $t = 0.005$ (red), $t = 0.01$ (blue) and $t = 0.015$ (green), where $\alpha = 0.1$ and $D = 1$. Numerical error creeps in when $t = 0.01$.

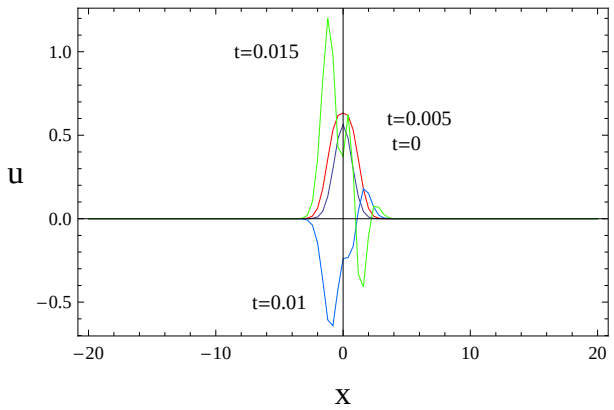

Figure 31: Numerical solutions for fractional time Cattaneo equation (4.1) for $t = 0$ (black), $t = 0.005$ (red), $t = 0.01$ (blue) and $t = 0.015$ (green), where $\alpha = 0.1$ and $D = 1.5$. The system is unstable due to numerical error.

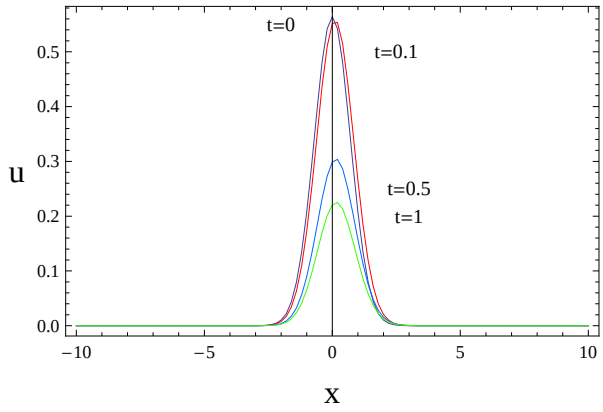

Figure 32: Numerical solutions for fractional time Cattaneo equation (4.1) where $\alpha = 0.5$ and $D = 0.1$. Volume is not conserved from the behaviour over time $t = 0$ (black), $t = 0.1$ (red), $t = 0.5$ (blue) and $t = 1$ (green).

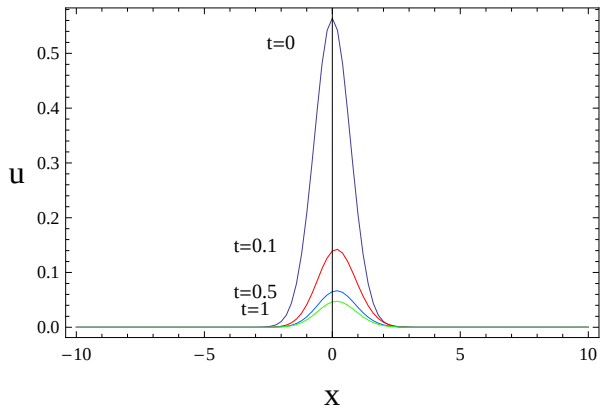

Figure 33: Numerical solutions for fractional time Cattaneo equation (4.1) over times $t = 0$ (black), $t = 0.1$ (red), $t = 0.5$ (blue) and $t = 1$ (green), where $\alpha = 0.5$ and $D = 0.5$. Diffusive behaviour is observed faster than when $D = 0.1$.

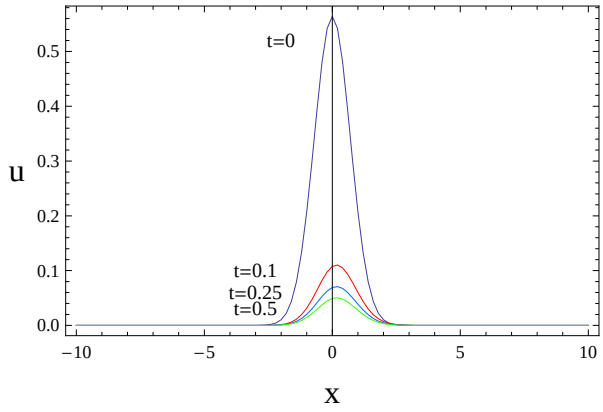

Figure 34: Numerical solutions for fractional time Cattaneo equation (4.1) for $t = 0$ (black), $t = 0.1$ (red), $t = 0.25$ (blue) and $t = 0.5$ (green), where $\alpha = 0.5$ and $D = 1$. Solution shows diffusive behaviour.

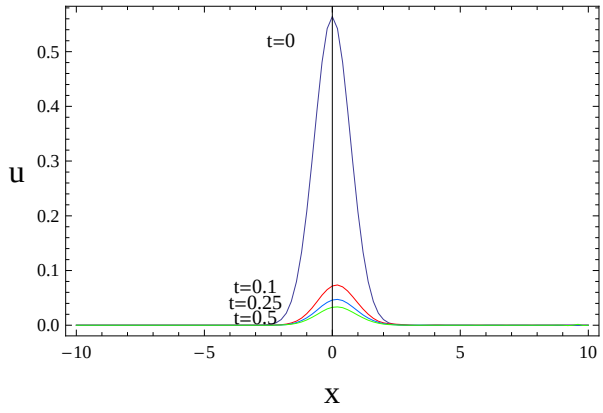

Figure 35: Numerical solutions for fractional time Cattaneo equation (4.1) for for $t = 0$ (black), $t = 0.1$ (red), $t = 0.25$ (blue) and $t = 0.5$ (green) where $\alpha = 0.5$ and $D = 1.5$. Solution shows diffusive behaviour faster than when $D = 1$.

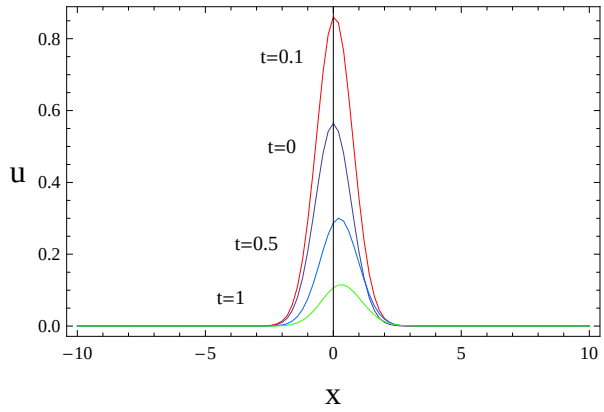

Figure 36: Numerical solutions for fractional time Cattaneo equation (4.1) where $\alpha = 0.9$ and $D = 0.1$. The system reverts to diffusive behaviour after $t = 0.1$ (red), as shown at $t = 0.5$ (blue) and $t = 1$ (green)

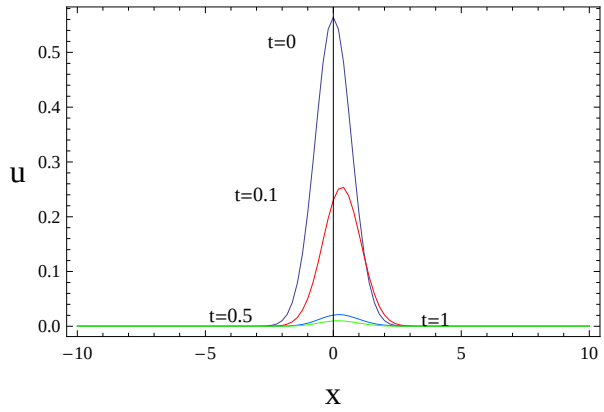

Figure 37: Numerical solutions for fractional time Cattaneo equation (4.1) where $\alpha = 0.9$ and $D = 0.5$. Diffusive behaviour is shown over times $t = 0$ (black), $t = 0.1$ (red), with rapid diffusion at $t = 0.5$ (blue) and $t = 1$ (green).

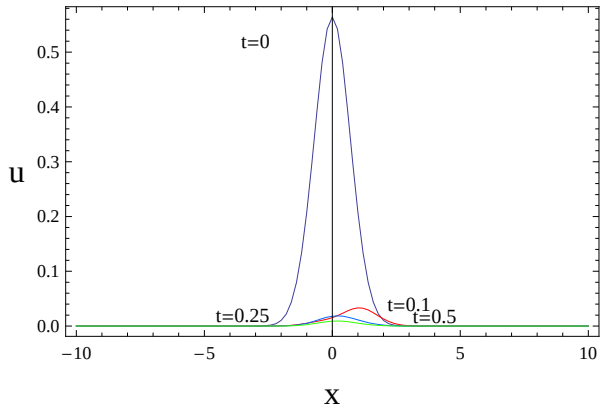

Figure 38: Numerical solutions for fractional time Cattaneo equation (4.1) where $\alpha = 0.9$ and $D = 1$. Diffusive behaviour is shown over times $t = 0$ (black), $t = 0.1$ (red), with rapid diffusion at $t = 0.5$ (blue) and $t = 1$ (green).

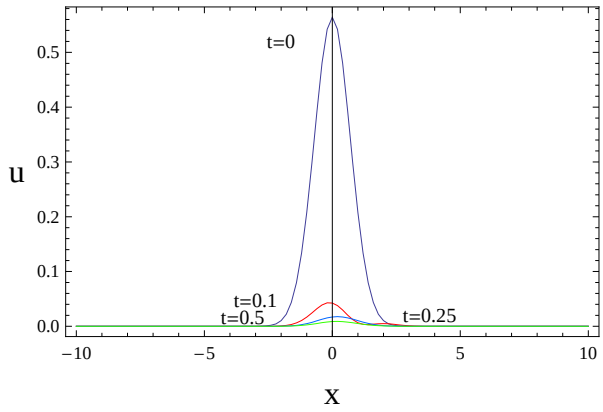

Figure 39: Numerical solutions for fractional time Cattaneo equation (4.1) where $\alpha = 0.9$ and $D = 1.5$. Diffusive behaviour is shown over times $t = 0$ (black), $t = 0.1$ (red), with rapid diffusion at $t = 0.5$ (blue) and $t = 1$ (green).

In the case of $\alpha = 0.5$, $D = 1$; $\alpha = 0.5$, $D = 1.5$ and $\alpha = 0.9$, $D = 1.5$ (Figure 34, 35, 39) solutions have been calculated using $\Delta t = 0.005$ and plotted over times $t = 0, 0.1, 0.25, 0.5$ to show diffusive behaviour. We observe in Figure 34 and 35 diffusive behaviour occurs faster for lower values for D. In Figure 39 we observe rapid diffusive behaviour when compared to solutions for lower values of α. Solutions for $\alpha = 0.1$, $D = 0.5$ were calculated with $\Delta t = 0.005$ (Figure 29) and plotted over the interval $[-20, 20]$, for smaller intervals the boundary conditions are not satisfied. Diffusive behaviour is observed to occur slower. Solutions for $\alpha = 0.1$, $D = 0.5$ and $\alpha = 0.1$, $D = 1.5$ are observed as unstable with $\Delta = 0.005, 0.01$. For $t > 0.005$ numerical error is large and the system becomes more unstable (Figure 30, 31).

4.2 Fractional space Cattaneo equation

Consider the space β-order fractional partial differential equation which is a combination of a fractional space derivative operating on time

$$\frac{\partial u}{\partial t} = D\frac{\partial^\beta u}{\partial x^\beta} - \tau\frac{\partial^\beta}{\partial x^\beta}\left(\frac{\partial u}{\partial t}\right), \tag{4.4}$$

where $1 < \beta \leq 2$, D is the diffusion coefficient and $\tau \ll 1$.

As previously carried out for the fractional space diffusion equation we apply a forward difference approximation to the time derivative and the right-shifted Grünwald formula (3.6) with a Crank-

Nicholson average over time to the β-order fractional derivative. Thus

$$\begin{aligned}\frac{1}{\Delta t}(u_i^{j+1}-u_i^j) = \frac{D}{(2\Delta x)^\beta}\left(\sum_{k=0}^{i+1} g_{\beta,k}u_{i-k+1}^{j+1} + \sum_{k=0}^{i+1} g_{\beta,k}u_{i-k+1}^{j}\right) \\ -\frac{\tau}{2\Delta t(\Delta x)^\beta}\left(\sum_{k=0}^{i+1} g_{\beta,k}u_{i-k+1}^{j+1} - \sum_{k=0}^{i+1} g_{\beta,k}u_{i-k+1}^{j}\right).\end{aligned} \tag{4.5}$$

We rearrange and simplify equation (4.5) to the following difference equation to be solved

$$u_i^{j+1} + (\gamma-\lambda)\sum_{k=0}^{i+1} g_{\beta,k}u_{i-k+1}^{j+1} = u_j^i + (\gamma+\lambda)\sum_{k=0}^{i+1} g_{\beta,k}u_{i-k+1}^{j}, \tag{4.6}$$

where $\lambda = \dfrac{D\Delta t}{2(\Delta x)^\beta}$ and $\gamma = \dfrac{\tau}{2(\Delta x)^\beta}$.

We expand and simplify the left-hand side of (4.6)

$$(\gamma-\lambda)g_{\beta,0}u_{i+1}^{j+1} + (1+(\gamma-\lambda)g_{\beta,1})u_i^{j+1} + (\gamma-\lambda)g_{\beta,2}u_{i-1}^{j+1} + \cdots + (\gamma-\lambda)g_{\beta,i}u_1^{j+1} + (\gamma-\lambda)g_{\beta,i+1}u_0^{j+1}.$$

Similarly we expand and simplify the right-hand side of (4.6)

$$(\gamma+\lambda)g_{\beta,0}u_{i+1}^{j}+(1+(\gamma+\lambda)g_{\beta,1})u_i^{j}+(\gamma+\lambda)g_{\beta,2}u_{i-1}^{j}+\cdots+(\gamma+\lambda)g_{\beta,i}u_1^{j}+(\gamma+\lambda)g_{\beta,i+1}u_0^{j}.$$

After applying the boundary condition the matrix form of the problem to be solved at the time step t_{j+1} is

$$\underline{u}^{j+1} = L^{-1}R\underline{u}^{j},$$

where

$$L = \begin{pmatrix} 1 & 0 & \dots & \dots & \dots & \dots & \dots & 0 \\ (\gamma-\lambda)g_{\beta,2} & (1+(\gamma-\lambda)g_{\beta,1} & (\gamma-\lambda)g_{\beta,0} & 0 & \dots & \dots & \dots & 0 \\ (\gamma-\lambda)g_{\beta,3} & (\gamma-\lambda)g_{\beta,2} & (1+(\gamma-\lambda)g_{\beta,1} & (\gamma-\lambda)g_{\beta,0} & 0 & \dots & \dots & 0 \\ \vdots & \ddots & \ddots & \vdots & \vdots & \vdots & \vdots & \vdots \\ \vdots & \vdots & \ddots & \ddots & \vdots & \vdots & \vdots & \vdots \\ \vdots & \vdots & \vdots & \ddots & \ddots & \vdots & \vdots & \vdots \\ (\gamma-\lambda)g_{\beta,n} & (\gamma-\lambda)g_{\beta,n-1} & \dots & \dots & \dots & (\gamma-\lambda)g_{\beta,2} & (1+(\gamma-\lambda)g_{\beta,1}) & (\gamma-\lambda)g_{\beta,0} \\ 0 & 0 & \dots & \dots & \dots & \dots & 0 & 1 \end{pmatrix},$$

$$R = \begin{pmatrix} 1 & 0 & \dots & \dots & \dots & \dots & \dots & 0 \\ (\gamma+\lambda)g_{\beta,2} & (1+(\gamma+\lambda)g_{\beta,1}) & (\gamma+\lambda)g_{\beta,0} & 0 & \dots & \dots & \dots & 0 \\ (\gamma+\lambda)g_{\beta,3} & (\gamma+\lambda)g_{\beta,2} & (1+(\gamma+\lambda)g_{\beta,1}) & (\gamma+\lambda)g_{\beta,0} & 0 & \dots & \dots & 0 \\ \vdots & \ddots & \ddots & \vdots & \vdots & \vdots & \vdots & \vdots \\ \vdots & \vdots & \ddots & \ddots & \vdots & \vdots & \vdots & \vdots \\ \vdots & \vdots & \vdots & \ddots & \ddots & \vdots & \vdots & \vdots \\ (\gamma+\lambda)g_{\beta,n} & (\gamma+\lambda)g_{\beta,n-1} & \dots & \dots & \dots & (\gamma+\lambda)g_{\beta,2} & (1+(\gamma+\lambda)g_{\beta,1}) & (\gamma+\lambda)g_{\beta,0} \\ 0 & 0 & \dots & \dots & \dots\dots & & 0 & 1 \end{pmatrix},$$

with $\underline{u}^{j+1}$ and $\underline{u}^{j}$ defined previously.

We determine solutions for $D = 0.1, 0.5, 1, 1.5$ and $\beta = 1.2, 1.5, 1.9$ for each value of D at times $t = 0, 5, 10, 20$, over the interval $[-50, 50]$ to sufficiently depict the behaviours observed.

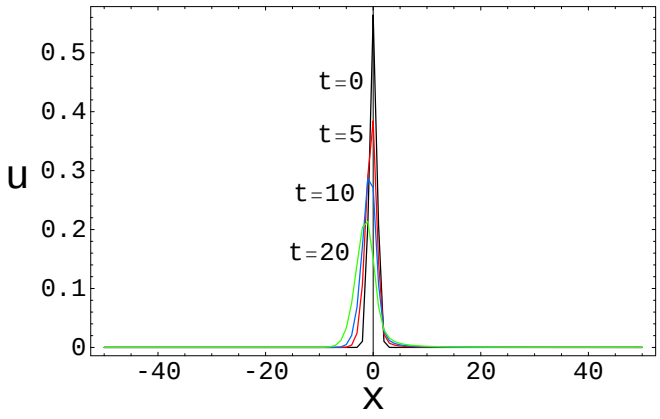

Figure 40: Numerical solutions for fractional space Cattaneo equation (4.4) for $t = 0$ (black), $t = 0.1$ (red), $t = 0.5$ (blue) and $t = 1$ (green), where $\beta = 1.2$ and $D = 0.1$. Results show normal diffusive behaviour.

Figures 40, 41, 42 and 43 depict the solution for the different values of D when $\beta = 1.2$. With $\beta = 1.5$ Figures 44, 45, 46 and 47 show the results for $D = 0.1, 0.5, 1, 1.5$ respectively. Similarly Figures 48, 49, 50 and 51 show results for $\beta = 1.9$. When $D = 0.1$ diffusion is slow. With higher values of β and D diffusion becomes faster. We observe similar results to those in Section 4.2. Results are skewed to the left (behaviour relating to the right-shifted Grüwald formula) for $\beta = 1.2, 1.5$ and display Gaussian normal distribution behaviour for $\beta = 1.9$.

In this chapter we have considered the numerical solutions for the fractional time Cattaneo and fractional space Cattaneo equations. Results obtained for the fractional time Cattaneo equations displayed slight propagation properties with unstable results for

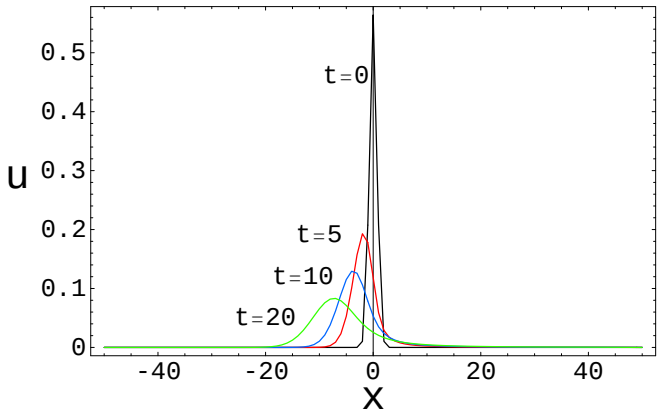

Figure 41: Numerical solutions for fractional space Cattaneo equation (4.4) where $\beta = 1.2$ and $D = 0.5$. Results are shown at $t = 0$ (black), $t = 0.1$ (red), $t = 0.5$ (blue) and $t = 1$ (green), normal diffusive behaviour is observed, but skewed to the left.

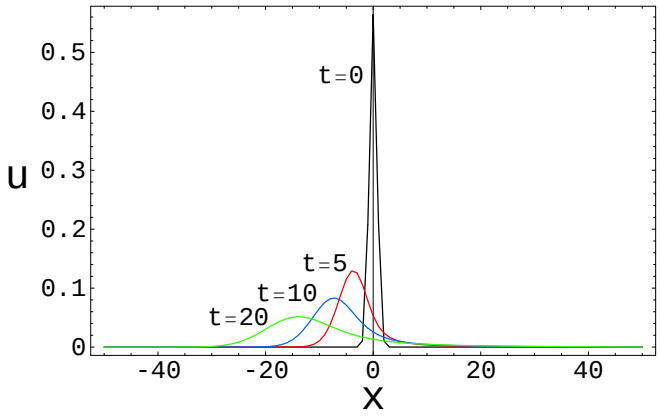

Figure 42: Numerical solutions for fractional space Cattaneo equation (4.4) where $\beta = 1.2$ and $D = 1$. Results are shown at $t = 0$ (black), $t = 0.1$ (red), $t = 0.5$ (blue) and $t = 1$ (green), normal diffusive behaviour is observed faster than in Figure 41, but skewed to the left.

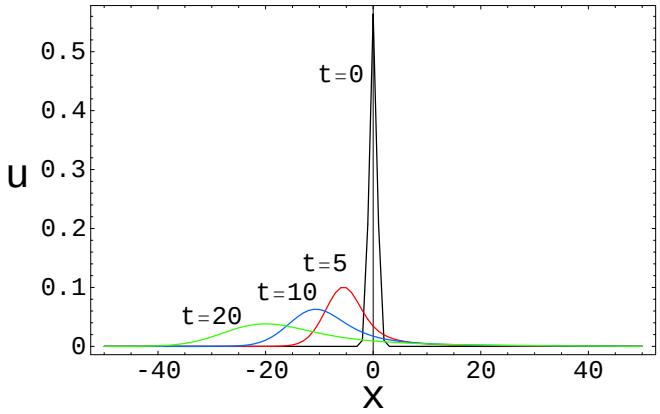

Figure 43: Numerical solutions for fractional space Cattaneo equation (4.4) where $\beta = 1.2$ and $D = 1.5$. Results are shown at $t = 0$ (black), $t = 0.1$ (red), $t = 0.5$ (blue) and $t = 1$ (green), normal diffusive behaviour is observed faster than in Figures 41 and 42, but skewed to the left.

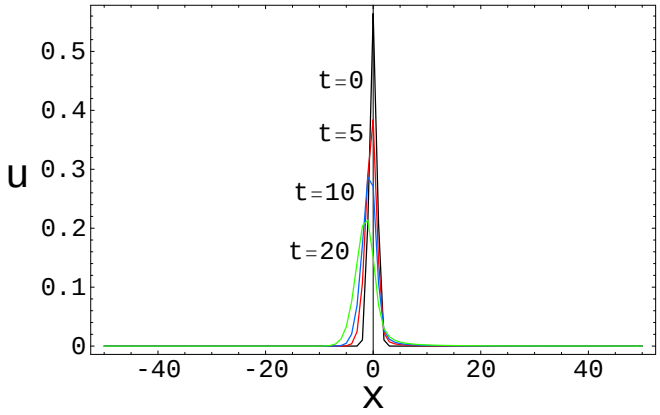

Figure 44: Numerical solutions for fractional space Cattaneo equation (4.4) for $t = 0$ (black), $t = 0.1$ (red), $t = 0.5$ (blue) and $t = 1$ (green), where $\beta = 1.5$ and $D = 0.1$. Normal diffusive behaviour is observed.

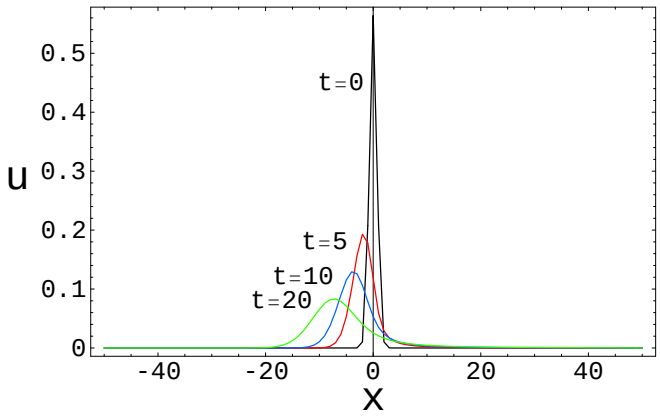

Figure 45: Numerical solutions for fractional space Cattaneo equation (4.4) for $t = 0$ (black), $t = 0.1$ (red), $t = 0.5$ (blue) and $t = 1$ (green), where $\beta = 1.5$ and $D = 0.5$. Diffusive behaviour is observed skewed to the left.

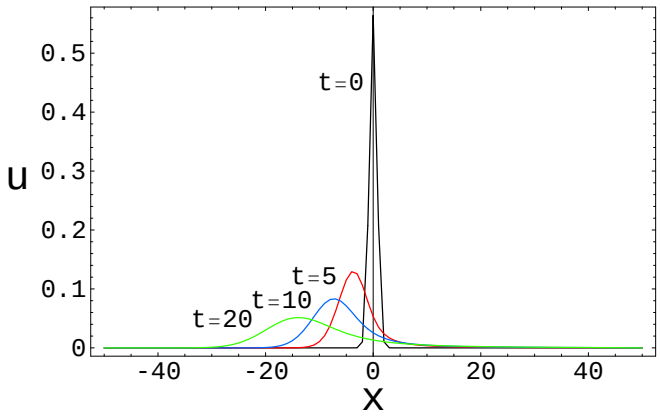

Figure 46: Numerical solutions for fractional space Cattaneo equation (4.4) where $\beta = 1.5$ and $D = 1$. Superdiffusive behaviour is observed skewed to the left at times $t = 0$ (black), $t = 0.1$ (red), $t = 0.5$ (blue) and $t = 1$ (green).

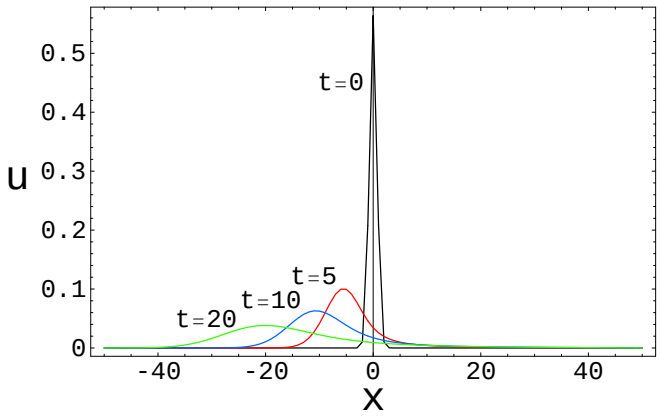

Figure 47: Numerical solutions for fractional space Cattaneo equation (4.4) where $\beta = 1.5$ and $D = 1.5$. Superdiffusive behaviour is observed skewed to the left at times $t = 0$ (black), $t = 0.1$ (red), $t = 0.5$ (blue) and $t = 1$ (green).

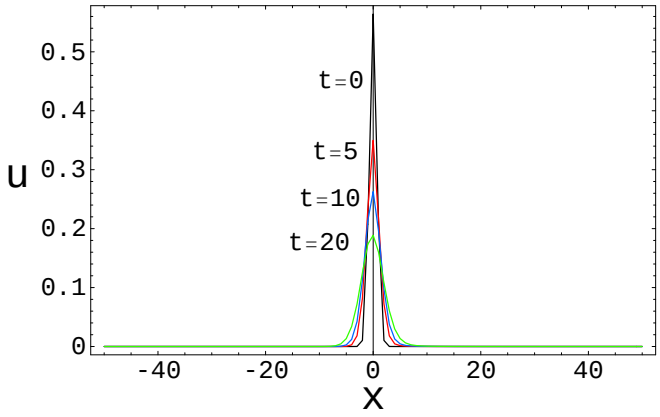

Figure 48: Numerical solutions for fractional space Cattaneo equation (4.4) for $t = 0$ (black), $t = 0.1$ (red), $t = 0.5$ (blue) and $t = 1$ (green), where $\beta = 1.9$ and $D = 0.1$. Normal diffusive behaviour is observed with a normal distribution.

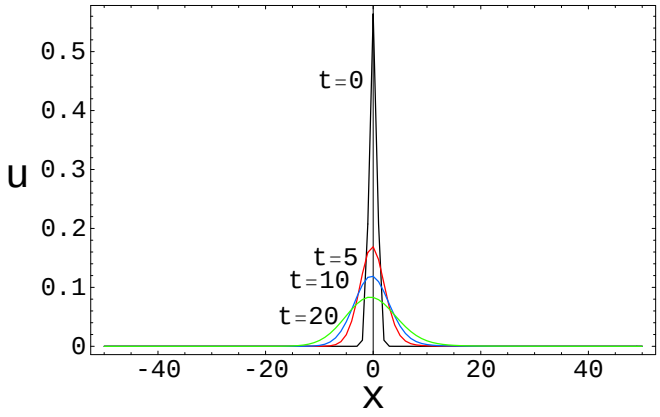

Figure 49: Numerical solutions for fractional space Cattaneo equation (4.4) where $\beta = 1.9$ and $D = 0.5$. Results are shown at times $t = 0$ (black), $t = 0.1$ (red), $t = 0.5$ (blue) and $t = 1$ (green) showing superdiffusive behaviour.

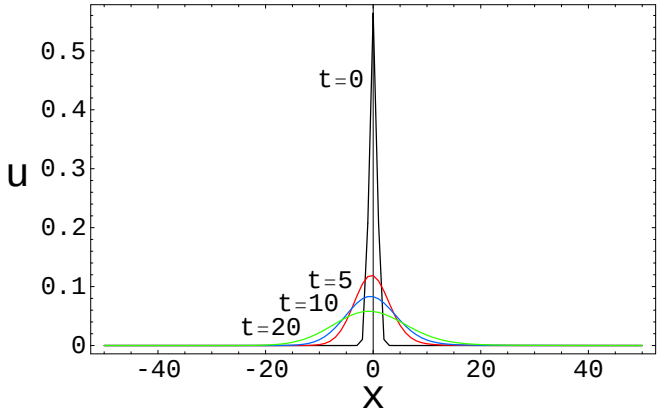

Figure 50: Numerical solutions for fractional space Cattaneo equation (4.4) where $\beta = 1.9$ and $D = 1$. Results are shown at times $t = 0$ (black), $t = 0.1$ (red), $t = 0.5$ (blue) and $t = 1$ (green) showing superdiffusive behaviour.

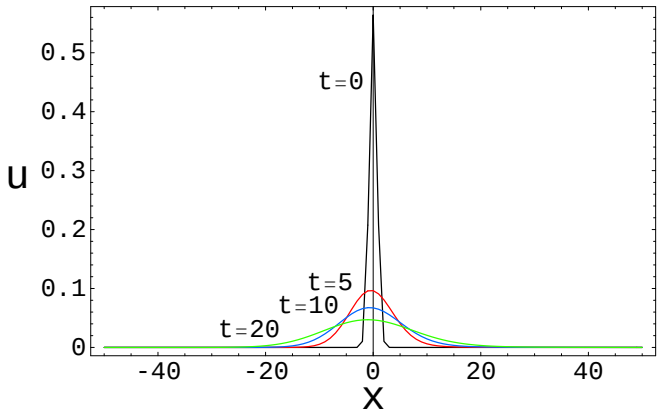

Figure 51: Numerical solutions for fractional space Cattaneo equation (4.4) where $\beta = 1.9$ and $D = 1.5$. Results are shown at times $t = 0$ (black), $t = 0.1$ (red), $t = 0.5$ (blue) and $t = 1$ (green) showing superdiffusive behaviour.

$D = 1, 1.5$ when $\alpha = 0.1$. The results for the fractional space Cattaneo equation were all stable and displayed strong properties of propagation, with the direction of propagation dependent on the sign of the extra term that is multiplied by τ.

5 Concluding remarks and possible future work

In this chapter we compare the numerical solutions for equations (3.1), (3.2), (3.5), (4.1) and (4.4) at $t = 0.5$ where $D = 0.5$, $\alpha = 0.5$ and $\beta = 1.9$ over the interval $[-10, 10]$. We compare where possible (excluding oscillatory / unstable behaviour) the effects of the different values of the order of our equations with the solutions obtained (i.e. we compare the different results obtained when using different α's and β's).

We also compare the effects of different diffusion coefficients on the solutions. Numerical results are shown graphically. These plots show the behaviour of the MSD and we interpret them as telling us how the particles in the system behave, from which we make conclusions. This chapter concludes with a brief look at recent work and possible future work.

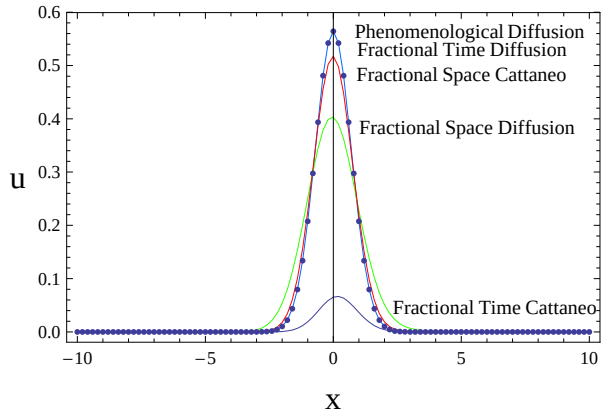

Figure 52: Numerical solutions for equations (3.1), (3.2), (3.5), (4.1) and (4.4) at $t = 0.5$ where $D = 0.5$, $\alpha = 0.5$ and $\beta = 1.9$. We observe similar behaviour for the phenomenological diffusion (3.2) (dotted) and fractional time diffusion equation (3.1) (blue). Fractional space Cattaneo (4.4) (red) and fractional space diffusion (3.5) (green) solutions show faster diffusive behaviour, with fractional time Cattaneo equation (4.1) (black) showing rapid diffusive behaviour.

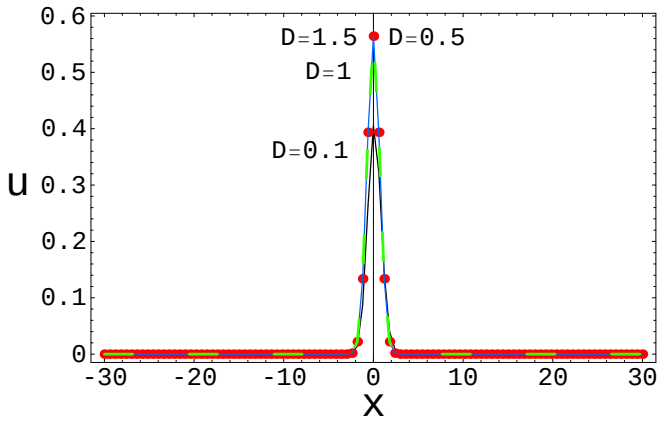

Figure 53: Numerical solutions for fractional time diffusion equation (3.1) at $t = 1$ where $\alpha = 0.1$. Solution is plotted for $D = 0.1$ (black), $D = 0.5$ (dotted red), $D = 1$ (blue) and $D = 1.5$ (dashed green). Results are consistent for $D = 0.5$, $D = 1$ and $D = 1.5$.

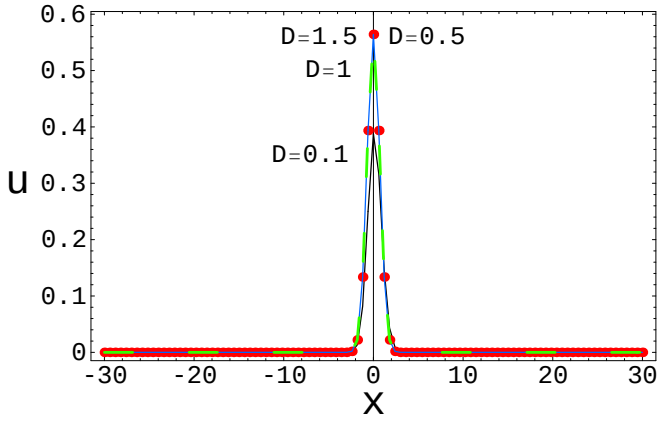

Figure 54: Numerical solutions for fractional time diffusion equation (3.1) at $t = 1$ where $\alpha = 0.5$. Solution is plotted for $D = 0.1$ (black), $D = 0.5$ (dotted red), $D = 1$ (blue) and $D = 1.5$ (dashed green). Results are consistent for $D = 0.5$, $D = 1$ and $D = 1.5$.

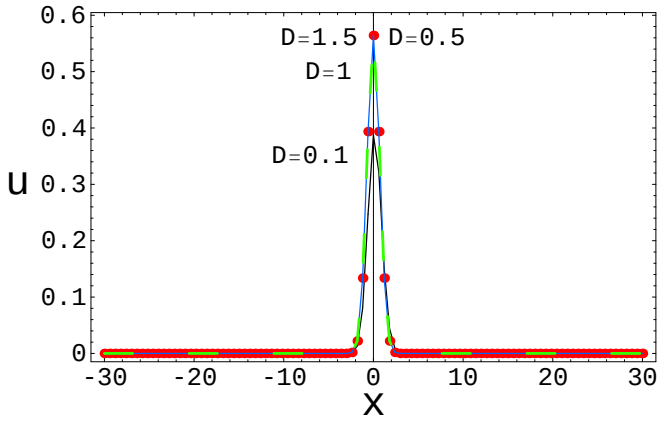

Figure 55: Numerical solutions for fractional time diffusion equation (3.1) at $t = 1$ where $\alpha = 0.9$. Solution is plotted for $D = 0.1$ (black), $D = 0.5$ (dotted red), $D = 1$ (blue) and $D = 1.5$ (dashed green). Results are consistent for $D = 0.5$, $D = 1$ and $D = 1.5$.

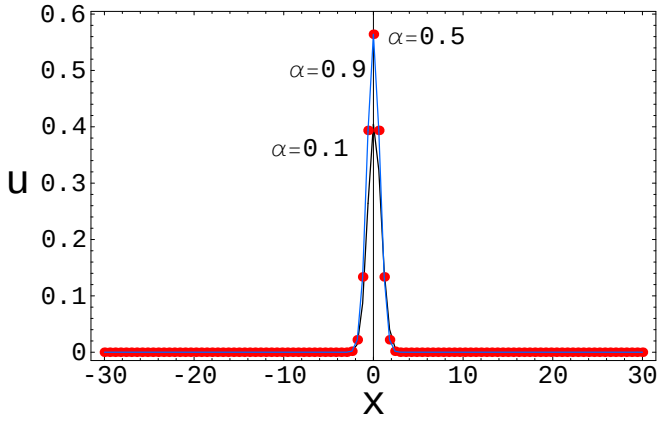

Figure 56: Numerical solutions for fractional time diffusion equation (3.1) at $t = 1$ where $D = 0.1$. Different values for α are shown where $\alpha = 0.1$ (black), $\alpha = 0.5$ (dotted red) and $\alpha = 0.9$ (blue). Results are consistent for $\alpha = 0.5$ and $\alpha = 0.9$.

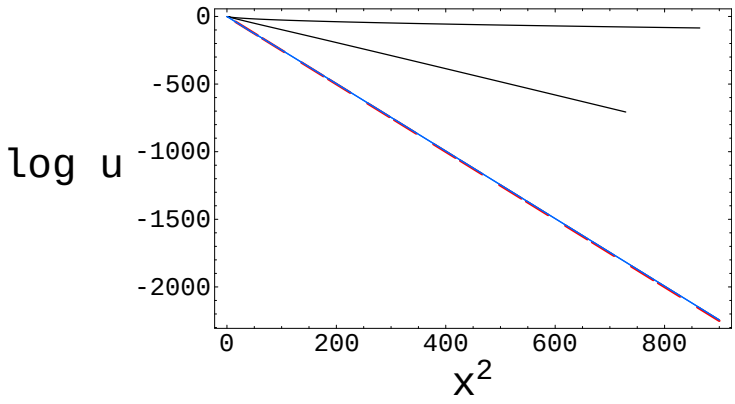

Figure 57: Numerical solutions for the MSD of fractional time diffusion equation (3.1) at $t = 1$ where $D = 0.1$ and $\alpha = 0.1$ (black). Compare this to MSD of the analytical diffusion equation (3.2) (dashed red) and the analytical Cattaneo equation (4.2) (blue). Results are consistent to anomalous diffusive behaviour.

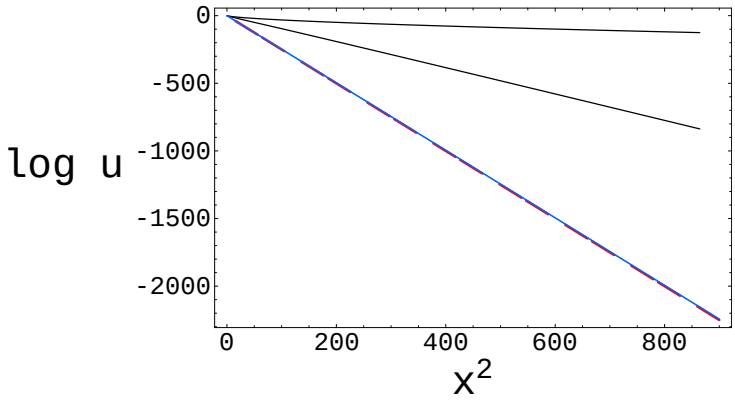

Figure 58: Numerical solutions for the MSD of fractional time diffusion equation (3.1) at $t = 1$ where $D = 0.1$ and $\alpha = 0.5$ (black). Compare this to MSD of the analytical diffusion equation (3.2) (dashed red) and the analytical Cattaneo equation (4.2) (blue). Results are consistent to anomalous diffusive behaviour.

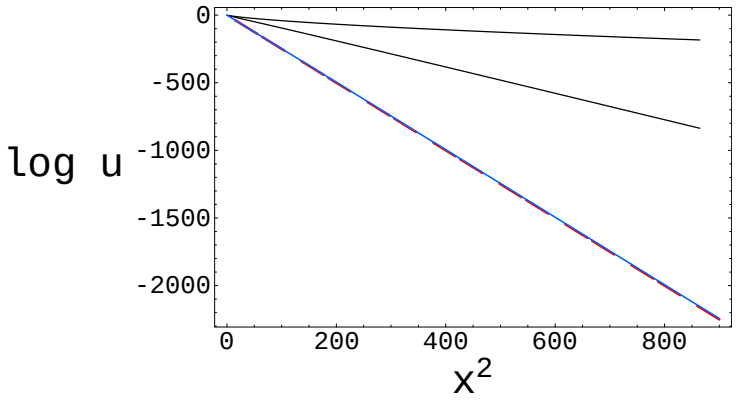

Figure 59: Numerical solutions for the MSD of fractional time diffusion equation (3.1) at $t = 1$ where $D = 0.1$ and $\alpha = 0.9$ (black). Compare this to MSD of the analytical Diffusion equation (3.2) (dashed red) and the analytical Cattaneo equation (4.2) (blue). Results are consistent to anomalous diffusive behaviour.

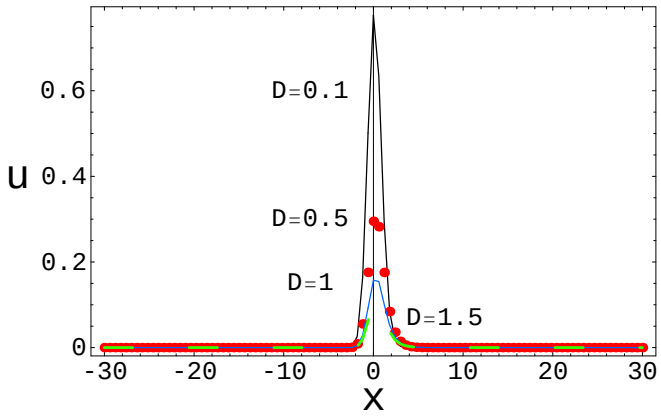

Figure 60: Numerical solutions for fractional time Cattaneo equation (4.1) at $t = 1$ where $\alpha = 0.5$. Different values for D are shown where $D = 0.1$ (black), $D = 0.5$ (dotted red), $D = 1$ (blue) and $D = 1.5$ (dashed green). Results are consistent for $D = 1$ and $D = 1.5$.

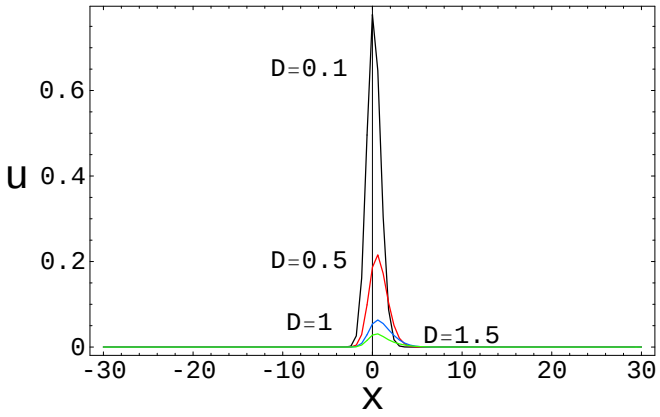

Figure 61: Numerical solutions for fractional time Cattaneo equation (4.1) at $t = 1$ where $\alpha = 0.9$. Different values for D are shown where $D = 0.1$ (black), $D = 0.5$ (red), $D = 1$ (blue) and $D = 1.5$ (green). Results show superdiffusion (for $D > 0.1$.

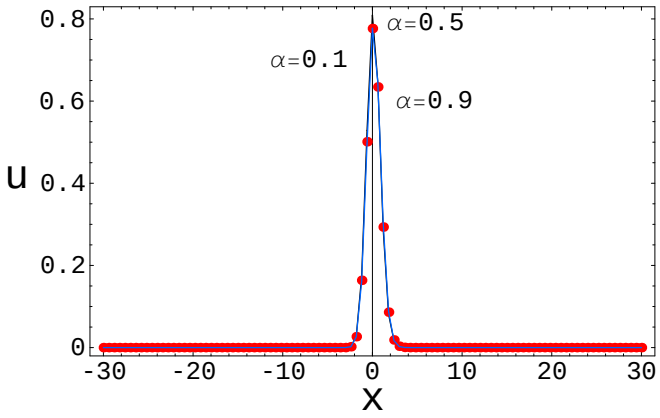

Figure 62: Numerical solutions for fractional time Cattaneo equation (4.1) at $t = 1$ where $D = 0.1$. Different values for α are shown where $\alpha = 0.1$ (black), $\alpha = 0.5$ (dotted red) and $\alpha = 0.9$ (blue). Results are consistent for all values of α.

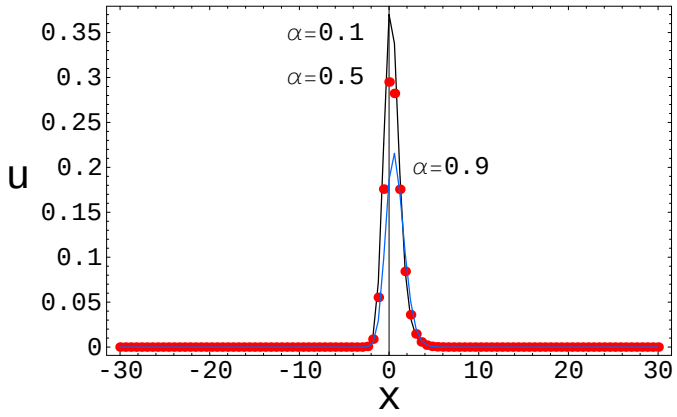

Figure 63: Numerical solutions for fractional time Cattaneo equation (4.1) at $t = 1$ where $D = 0.5$. Different values for α are shown where $\alpha = 0.1$ (black), $\alpha = 0.5$ (dotted red) and $\alpha = 0.9$ (blue). Increasing α has a superdiffusive effect.

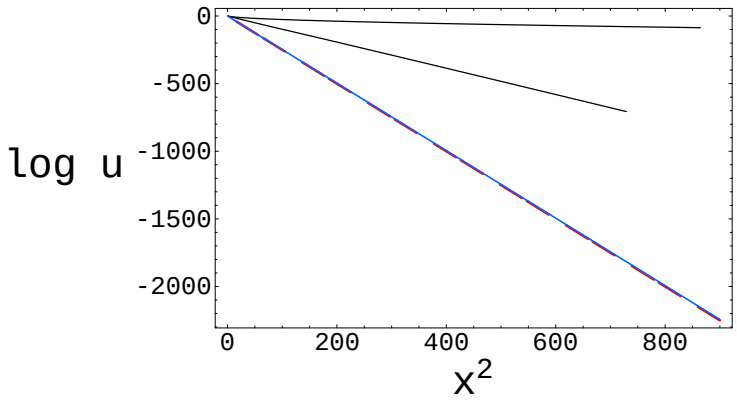

Figure 64: Numerical solutions for the MSD of fractional time Cattaneo equation (4.1) at $t = 1$ where $D = 0.1$ and $\alpha = 0.1$ (black). Compare this to MSD of the analytical diffusion equation (3.2) (dashed red) and the analytical Cattaneo equation (4.2) (blue). Results are consistent to anomalous diffusive behaviour.

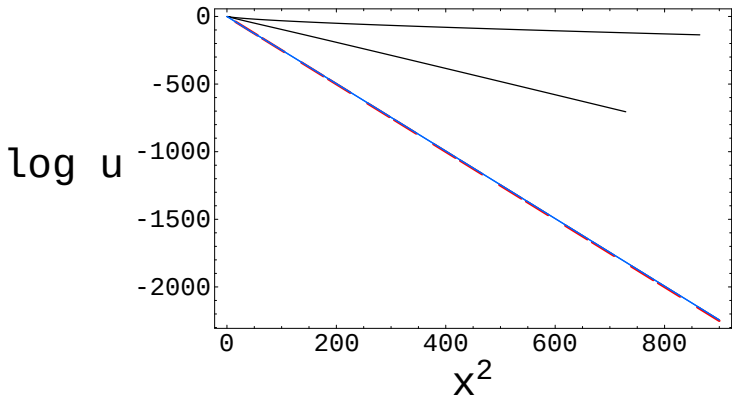

Figure 65: Numerical solutions for the MSD of fractional time Cattaneo equation (4.1) at $t = 1$ where $D = 0.1$ and $\alpha = 0.5$ (black). Compare this to MSD of the analytical diffusion equation (3.2) (dashed red) and the analytical Cattaneo equation (4.2) (blue). Results are consistent to anomalous diffusive behaviour.

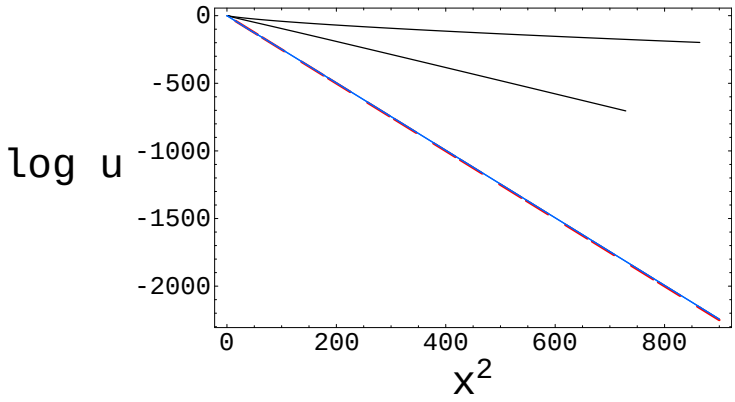

Figure 66: Numerical solutions for the MSD of fractional time Cattaneo equation (4.1) at $t = 1$ where $D = 0.1$ and $\alpha = 0.9$ (black). Compare this to MSD of the analytical diffusion equation (3.2) (dashed red) and the analytical Cattaneo equation (4.2) (blue). Results are consistent to anomalous diffusive behaviour.

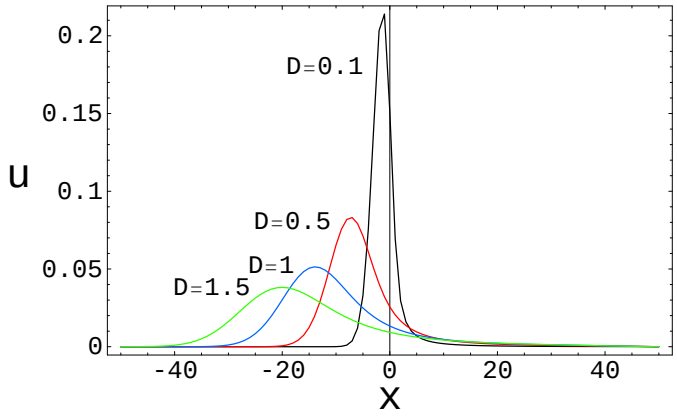

Figure 67: Numerical solutions for fractional space diffusion equation (3.5) at $t = 20$ where $\beta = 1.2$. Solution is plotted for $D = 0.1$ (black), $D = 0.5$ (red), $D = 1$ (blue) and $D = 1.5$ (green). Results are not consistent for different values of D and are skewed to the left.

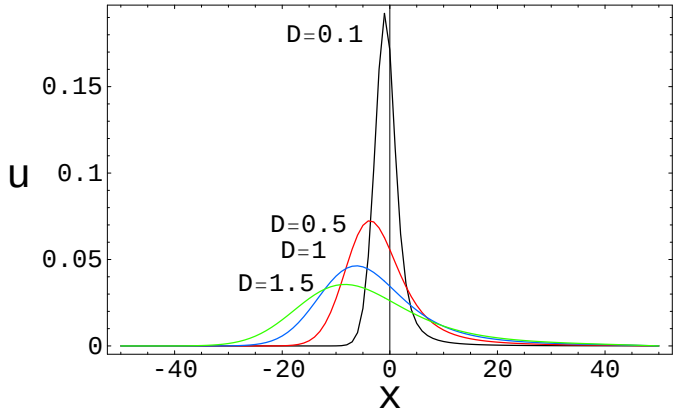

Figure 68: Numerical solutions for fractional space diffusion equation (3.5) at $t = 20$ where $\beta = 1.5$. Solution is plotted for $D = 0.1$ (black), $D = 0.5$ (red), $D = 1$ (blue) and $D = 1.5$ (green). Results are not consistent for different values of D and are skewed to the left.

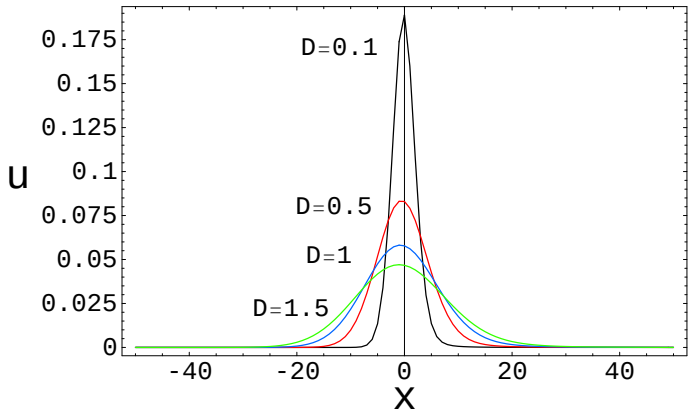

Figure 69: Numerical solutions for fractional space diffusion equation (3.5) at $t = 20$ where $\beta = 1.9$. Solution is plotted for $D = 0.1$ (black), $D = 0.5$ (red), $D = 1$ (blue) and $D = 1.5$ (green). Results are not consistent for different values of D and show a normal distribution.

Plotting the solutions for the fractional diffusion equations (equations (3.1), (3.5)) and fractional Cattaneo equations (equations (4.1), (4.4)) with the analytical solution of the phenomenological diffusion equation (3.2), we observe the behaviour of each equation (Figure 52). The fractional time Cattaneo equation exhibits rapid (superdiffusive) diffusive behaviour. The solutions to the fractional space diffusion and fractional space Cattaneo show diffusive behaviour that is faster than normal diffusion. We observe that the fractional time diffusion equation exhibits behaviour on par with normal diffusion (subdiffusive behaviour compared to equations (4.1), (4.4) and (3.5)).

In Figures 53, 54 and 55 we compare the results for $D = 0.1, 0.5, 1, 1.5$ for each $\alpha = 0.1, 0.5, 0.9$ for the fractional time diffusion equation.

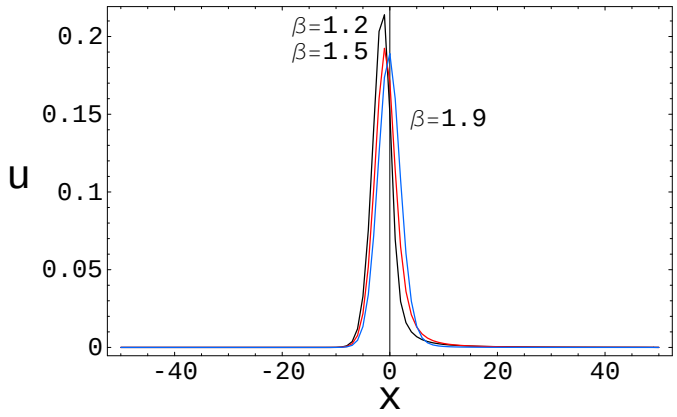

Figure 70: Numerical solutions for fractional space diffusion equation (3.5) at $t = 20$ where $D = 0.1$. Different values for β are shown where $\beta = 1.2$ (black), $\beta = 1.5$ (red) and $\beta = 1.9$ (blue). Numerical results for a smaller D appear almost consistent for different values of β.

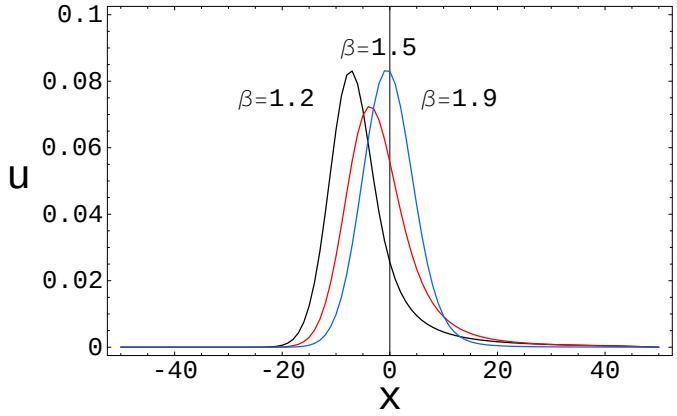

Figure 71: Numerical solutions for fractional space diffusion equation (3.5) at $t = 20$ where $D = 0.5$. Different values for β are shown where $\beta = 1.2$ (black), $\beta = 1.5$ (red) and $\beta = 1.9$ (blue). Results are not consistent for changing β when D is increased to 0.5.

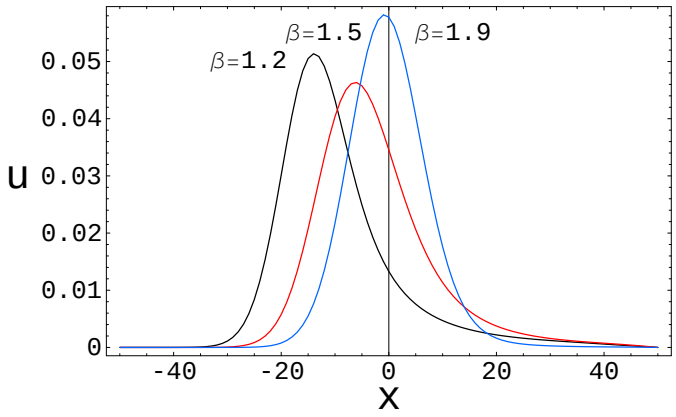

Figure 72: Numerical solutions for fractional space diffusion equation (3.5) at $t = 20$ where $D = 1$. Different values for β are shown where $\beta = 1.2$ (black), $\beta = 1.5$ (red) and $\beta = 1.9$ (blue). Results are not consistent for changing β when D is increased to 1.

For each α the results are consistent in showing that for a $D = 0.1$ the process of diffusion is faster, where the effects when $D = 0.5, 1.5$ are the same.

When these comparisons are made for the fractional time Cattaneo equation we notice a significant difference in the results for the different values of D when $\alpha = 0.5, 0.9$. Refer to Figures 60 and 61. For a lower diffusion coefficient diffusion occurs slower, while for higher values of the diffusion coefficient superdiffusion is observed. These observations are consistent for $\alpha = 0.5, 0.9$.

Comparing the effects of the different diffusion coefficients on the fractional space equations (both diffusion and Cattaneo) we observe

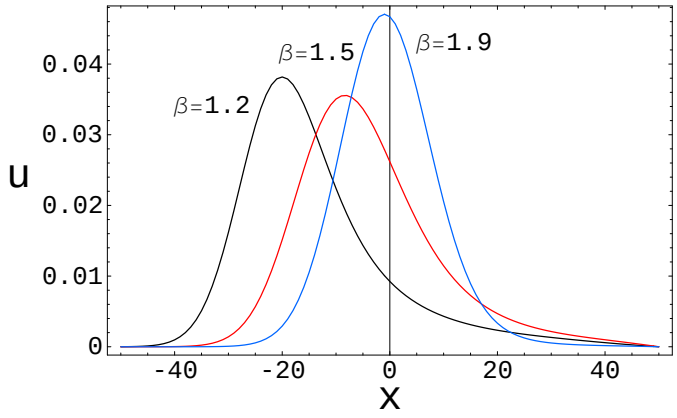

Figure 73: Numerical solutions for fractional space diffusion equation (3.5) at $t = 20$ where $D = 1.5$. Different values for β are shown where $\beta = 1.2$ (black), $\beta = 1.5$ (red) and $\beta = 1.9$ (blue). Results are not consistent for changing β when D is increased to 1.5.

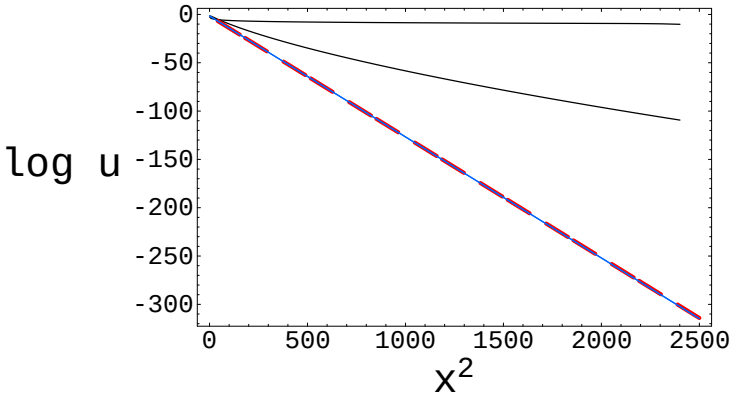

Figure 74: Numerical solutions for the MSD of fractional space diffusion equation (3.5) (black) at $t = 20$ where $D = 0.1$ and $\beta = 1.2$. Compare this to MSD of the analytical diffusion equation (3.2) (red dashed) and the analytical Cattaneo equation (4.2) (blue). Results are consistent to anomalous diffusive behaviour.

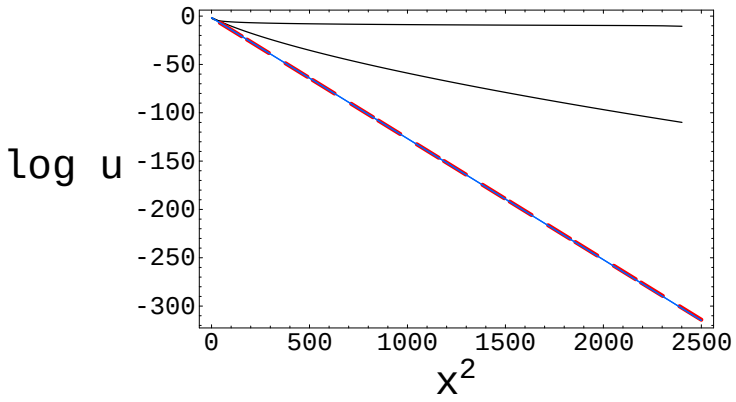

Figure 75: Numerical solutions for the MSD of fractional space diffusion equation (3.5) (black) at $t = 20$ where $D = 0.1$ and $\beta = 1.5$. Compare this to MSD of the analytical diffusion equation (3.2) (red dashed) and the analytical Cattaneo equation (4.2) (blue). Results are consistent to anomalous diffusive behaviour.

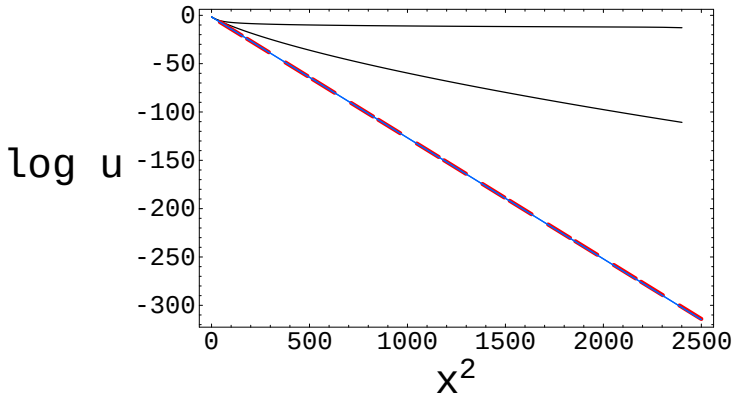

Figure 76: Numerical solutions for the MSD of fractional space diffusion equation (3.5) (black) at $t = 20$ where $D = 0.1$ and $\beta = 1.9$. Compare this to MSD of the analytical diffusion equation (3.2) (red dashed) and the analytical Cattaneo equation (4.2) (blue). Results are consistent to anomalous diffusive behaviour.

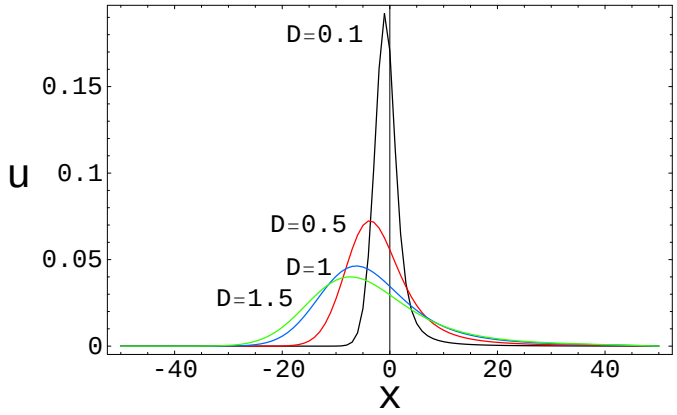

Figure 77: Numerical solutions for fractional space Cattaneo equation (4.4) at $t = 20$ where $\beta = 1.5$. Solution is plotted for $D = 0.1$ (black), $D = 0.5$ (red), $D = 1$ (blue) and $D = 1.5$ (green). Results show slightly skewed to the left and superdiffusion is observed.

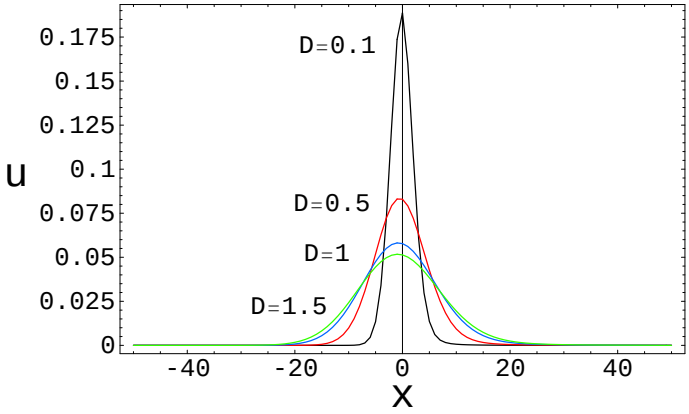

Figure 78: Numerical solutions for fractional space Cattaneo equation (4.4) at $t = 20$ where $\beta = 1.9$. Solution is plotted for $D = 0.1$ (black), $D = 0.5$ (red), $D = 1$ (blue) and $D = 1.5$ (green). Results show as a normal distribution and superdiffusion is observed.

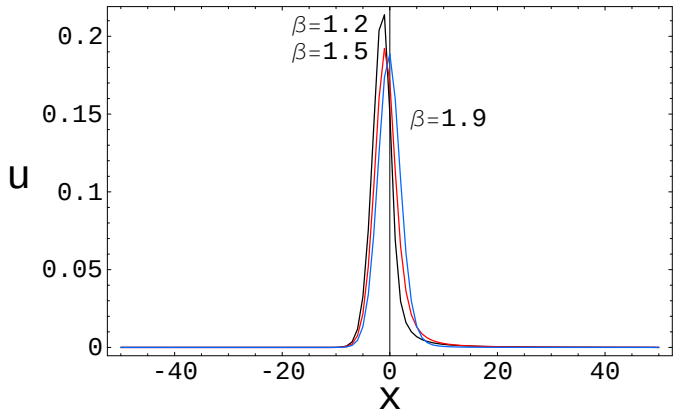

Figure 79: Numerical solutions for fractional space Cattaneo equation (4.4) at $t = 20$ where $D = 0.1$. Different values for β are shown where $\beta = 1.2$ (black), $\beta = 1.5$ (red) and $\beta = 1.9$ (blue). Numerical results for a smaller D appear almost consistent for different values of β.

the same or similar behaviour (Figures 67, 68, 77). When $D = 0.1$ diffusion occurs very slowly (subdiffusion), when $D = 0.5, 1, 1.5$ superdiffusion is observed. Results are displayed skewed to the left when $\beta = 1.2, 1.5$ but for $\beta = 1.9$ results follow a Gaussian behaviour with a more normal distribution (Figures 69 and 78).

Looking at the fractional time diffusion equation results, Figure 56, the results for the different values of α when $D = 0.1$, show superdiffusion for $\alpha = 0.1$ and are consistent with the results obtained for different diffusion coefficients.

Figures 62 and 63 compare the different values of α with $D = 0.1, 0.5$ for the fractional time Cattaneo equation. When $D = 0.1$ no change

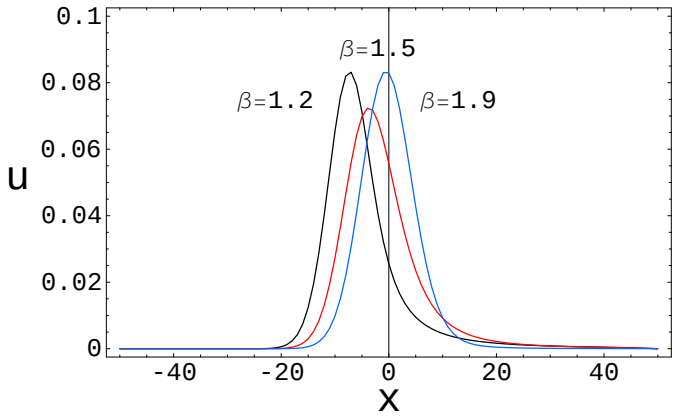

Figure 80: Numerical solutions for fractional space Cattaneo equation (4.4) at $t = 20$ where $D = 0.5$. Different values for β are shown where $\beta = 1.2$ (black), $\beta = 1.5$ (red) and $\beta = 1.9$ (blue). Results are not consistent for changing β when D is increased to 0.5.

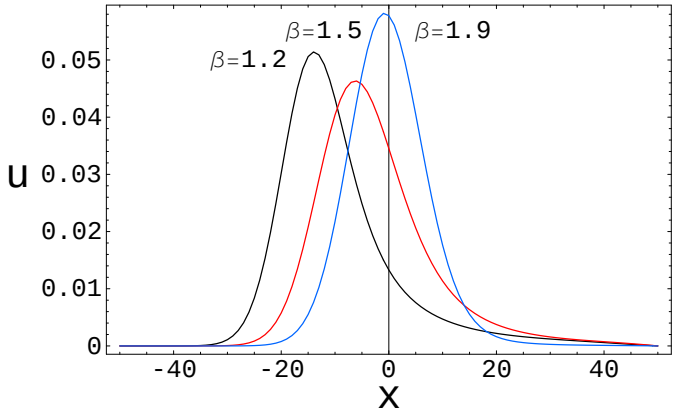

Figure 81: Numerical solutions for fractional space Cattaneo equation (4.4) at $t = 20$ where $D = 1$. Different values for β are shown where $\beta = 1.2$ (black), $\beta = 1.5$ (red) and $\beta = 1.9$ (blue). Results are not consistent for changing β when D is increased to 1.

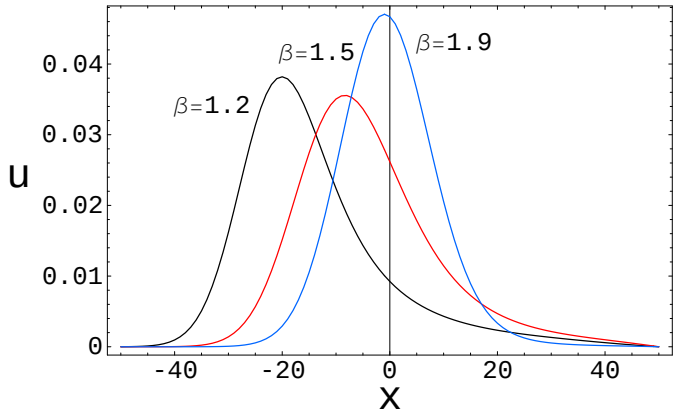

Figure 82: Numerical solutions for fractional space Cattaneo equation (4.4) at $t = 20$ where $D = 1.5$. Different values for β are shown where $\beta = 1.2$ (black), $\beta = 1.5$ (red) and $\beta = 1.9$ (blue). Results are not consistent for changing β when D is increased to 1.5.

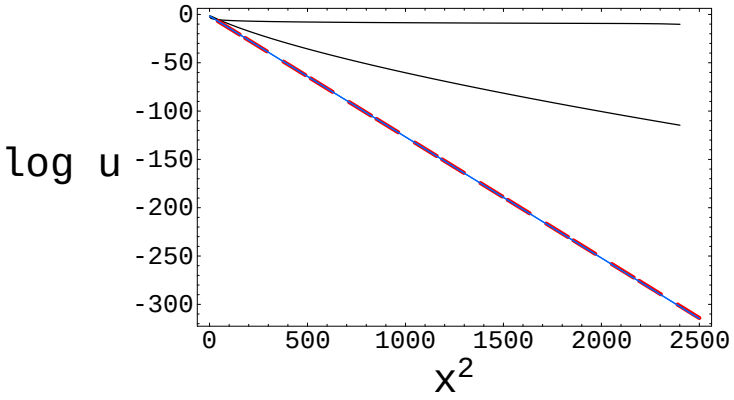

Figure 83: Numerical solutions for the MSD of fractional space Cattaneo equation (4.4) (black) at $t = 20$ where $D = 0.1$ and $\beta = 1.2$. Compare this to MSD of the analytical diffusion equation (3.2) (dashed red) and the analytical Cattaneo equation (4.2) (blue). Results are consistent to anomalous diffusive behaviour.

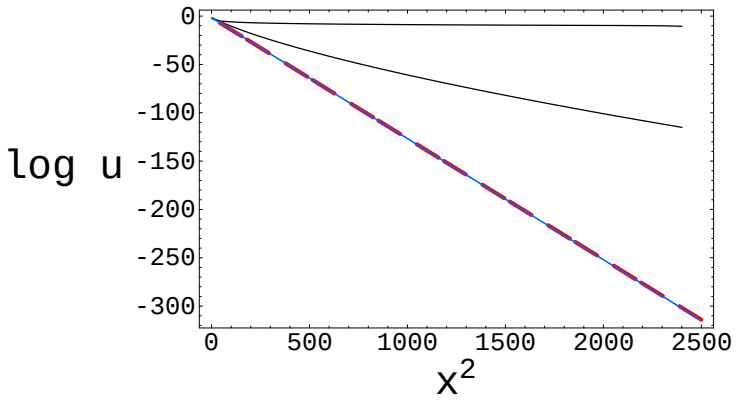

Figure 84: Numerical solutions for the MSD of fractional space Cattaneo equation (4.4) (black) at $t = 20$ where $D = 0.1$ and $\beta = 1.5$. Compare this to MSD of the analytical diffusion equation (3.2) (dashed red) and the analytical Cattaneo equation (4.2) (blue). Results are consistent to anomalous diffusive behaviour.

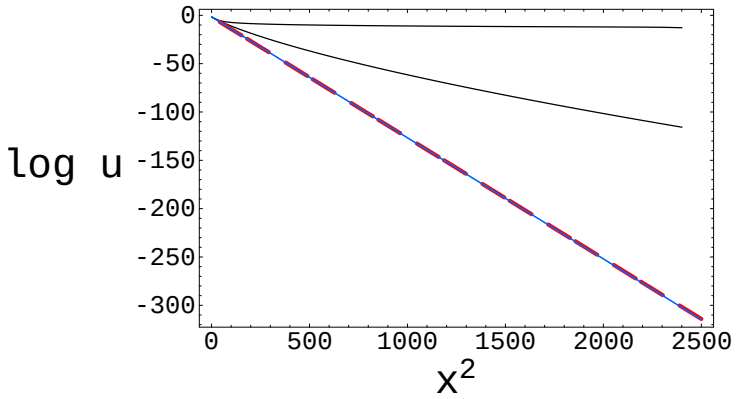

Figure 85: Numerical solutions for the MSD of fractional space Cattaneo equation (4.4) (black) at $t = 20$ where $D = 0.1$ and $\beta = 1.9$. Compare this to MSD of the analytical diffusion equation (3.2) (dashed red) and the analytical Cattaneo equation (4.2) (blue). Results are consistent to anomalous diffusive behaviour.

occurs in the results but when $D = 0.5$ lower values of α reflect subdiffusion, while larger values of α show superdiffusion.

Results comparing the effects of different values of β are similar for the fractional space diffusion equation and the fractional space Cattaneo equation. When $D = 0.1$ the results for $\beta = 1.2, 1.5, 1.9$ are almost consistent (Figure 70, 79). A significant difference between the results is observed when $D = 0.5, 1, 1.5$ (Figures 71, 72, 73, 80, 81, 82). We observe that for all the comparisons of the diffusion coefficients, when $\beta = 1.9$ results display Gaussian behaviour with a normal distribution while for other values of β results are skewed.

Figures 57, 58, 59, 64, 65 and 66 show the results when plotting the log of our numerical solutions against x^2 for the fractional time diffusion and for the fractional time Cattaneo equations $\alpha = 0.1, 0.5, 0.9$. Figures 74, 75, 76, 83, 84 and 85 show the log of the numerical solutions obtained for the fractional space diffusion and fractional space Cattaneo equations, with different values of β. To check for consistency each of these solutions is compared to the *log* of the analytical solutions of the diffusion equation (3.2) and the Cattaneo equation (4.2). All the figures show consistency to the log or MSD of equations (3.2) and (4.2), exhibiting superdiffusive behaviour (the slightly curved black lines as opposed to normal diffusive behaviour represented by the linear straight lines) for all the fractional time and space equations we have solved.

We observed that numerical solutions are unstable for a small fractional exponent ($\alpha = 0.1$) operating on the time derivative combined with larger values for the diffusivity coefficient (mainly $D = 1, 1.5$). Results that are stable are consistent to diffusive behaviour. When the fractional exponent is between 0 and 1 diffusion is slower, while when it is between 1 and 2 diffusion is faster. However, when the fractional exponent is combined with a lower diffusivity coefficient, the effect is subdiffusion.

Extensive work continues to be undertaken on fractional differential equations. Recent and common approaches for solving fractional differential equations are presented by Atanackovic and Stankovic [4], Momani and Odibat [37] and Erturk *et al* [45].

Atanackovic and Stankovic [4] take the approach of transforming a fractional differential system and converting it to a system of first-order ordinary differential equations. Yuan and Agrawal [47] have also investigated this approach, but have based it on a different definition of the fractional derivative. The results they obtain are in good agreement with results from other methods.

Momani and Odibat [37], and Erturk *et al* [45] have recently explored the use of a generalised Taylor formula and the GDTM (generalised differential transform method). They conclude that the methods investigated are efficient and convenient. Other papers explore the additional use of the Crank-Nicholson method in

discretizing fractional differential equations, which provides a stable and convergent solution [3, 1].

We have modeled the generalised Cattaneo equations and shown the numerical techniques used to solve these equations. These finite difference techniques have been applied to fractional diffusion and fractional Cattaneo equations. We have found that this approach works best for the equations where the fractional derivative operates on the spatial variable than for the equations where the fractional derivative operates on time. The interval points at which boundary conditions are imposed need to be chosen so that the fact that "no heat escapes" is satisfied (i.e. the fact that the ends of the rod mentioned in Section 1.1 are insulated). When the parameter $\Delta t = 0.01$ is halved, the fractional time Cattaneo scheme takes longer periods of time to run, however with a smaller time step the fractional time Cattaneo scheme can be run for a longer time period. To conclude the techniques applied are memory intensive and requires sufficient computational time with smaller spatial and time step lengths. This could be resolved with improvements in technology.

Possible work in the future includes investigating the Adomian approach for solving fractional differential equations as explored by Wazwaz and El-Sayed [46], and Odibat and Momani [38]. The advantage of the Adomian decomposition method is that solutions are provided in a rapid convergent series, with accuracy improving as

more terms of the approximate solution are computed. The accuracy, however, does depend on the fractional partial differential equation being solved. We could also investigate converting the partial differential equations to a system of first-order differential equations as presented by Atanackovic and Stankovic [4].

References

[1] M. M. Meerschaert, H. Scheffler and C. Tadjeran. Finite difference methods for two-dimensional fractional dispersion equation. *Journal of Computational Physics*, **211**: 249–261, 2006.

[2] A. Cartea and D. del-Castillo-Negrete. Fractional diffusion models of option prices in markets with jumps. *Physica A: Statistical Mechanics and its Applications*, **374**: 749–763, 2007.

[3] A. M. Abu-Saman and A. M. Assaf. Stability and Convergence of Crank-Nicholson Method for Fractional Advection Dispersion Equation. *Advances in Applied Mathematical Analysis*, **2**: 117–125, 2007.

[4] T.M. Atanackovic and B. Stankovic. On a numerical scheme for solving differential equations of fractional order. *Mechanics Research Communications*, **35**: 429–438, 2008.

[5] R. Balescu. V-langevin equations, continuous time random walks and fractional diffusion. *Chaos, Solitons and Fractals*, **34**: 62–80, 2007.

[6] A. Barletta and E. Zanchini. Unsteady heat conduction by internal-energy waves in solids. *Physical Review B*, **55**: 14208–14213, 1997.

[7] C. Tadjeran, M. M. Meerschaert and H. Scheffler. A second-order accurate numerical approximation for the fractional dif-

fusion equation. *Journal of Computational Physics*, **213**: 205–213, 2006.

[8] C. V. D. R. Anderson and K. K. Tamma. Novel heat conduction model for bridging different space and time scales. *Physical Review Letters*, **96**: 184301(1)–184301(4), 2006.

[9] C. Cattaneo. Sulla conduzione del calore. *Atti Sem. Mat. Fis. Univ. Modena*, **3**: 83–101, 1948.

[10] W. Chen and S. Holm. Physical interpretation of fractional diffusion-wave equation via lossy media obeying frequency power law. URL: http://arxiv.org/abs/math-ph/0303040, Simula Research Laboratory, 2003.

[11] A. Compte. Continuous time random walks on moving fluids. *Physical Review E*, **55**: 6821–6831, 1997.

[12] A. Compte and R. Metzler. The generalized cattaneo equation for the description of anomalous transport processes. *J. Phys. A: Math. Gen.*, **30**: 7277–7289, 1997.

[13] J. Crank. *The mathematics of diffusion*. Oxford University Press, Clarendon, 1975.

[14] D. G. Zill and M. R. Cullen. *Differential Equations with Boundary-Value Problems*. Brooks/Cole, Belmont, 2001.

[15] K. Diethelm and N. J. Ford. Numerical solutions of linear and non-linear fractional differential equations involving fractional derivatives of several orders. *Manchester Center for Compu-*

tational Mathematics Numerical Analysis Reports, **379**: 1–14, 2001.

[16] K. Diethelm and A. D. Freed. The FracPECE Subroutine for the Numerical Solution of Differential Equations of Fractional Order. In: S. Heinzel, T. Plesser (Eds.), Forschung und wissenschaftliches Rechnen 1998, Gesellschaft für Wisseschaftliche Datenverarbeitung, Göttingen, 1999, pp 57–71.

[17] A. Einstein. *Investigations on the Theory of the Brownian Movement*. Dover Publications, 1956.

[18] J. Gembarovic and V. Majernik. Determination of thermal parameters of relaxation materials. *International Journal of Heat Mass Transfer*, **30**: 199–201, 1987.

[19] J. Gembarovic and V. Majernik. Non-fourier propagation of heat pulses in finite medium. *International Journal of Heat Mass Transfer*, **31**: 1073–1081, 1988.

[20] P. Hanggi and F. Marchesoni. Introduction: 100 years of brownian motion. *Chaos*, **15**: 026101(1)–026101(5), 2005.

[21] R. Hilfer. On fractional dffusion and continuous time random walks. *Physica A: Statistical Mechanics and its Applications*, **329**: 35–40, 2003.

[22] D. D. Joseph and L. Preziosi. Heat waves. *Reviews of Modern Physics*, **61**: 41–73, 1989.

[23] D. D. Joseph and L. Preziosi. Addendum to the paper "Heat waves". *Reviews of Modern Physics*, **62**: 375–391, 1990.

[24] G. Jumarie. Stock exchange fractional dynamics defined as fractional exponential growth driven by (usual) Gaussian white noise. Application to fractional Black-Scholes equations. *Insurance: Mathematics and Economics*, **42**: 271–287, 2008.

[25] K. Diethelm, N. J. Ford and A. D. Freed. A predictor-corrector approach for the numerical solution of fractional differential equations. *Nonlinear Dynamics*, **29**: 3–22, 2002.

[26] K. E. Bassler, G. H. Gunaratne and J. L. McCauley. Markov processes, hurst exponents, and nonlinear diffusion equations: With application to finance. *Physica A: Statistical Mechanics and its Applications*, **369**: 343–353, 2006.

[27] L. R. da Silva, L. S. Lucena, E. K. Lenzi, R. S. Mendes and K. S. Fa. Fractional and nonlinear diffusion equation: additional results. *Physica A: Statistical Mechanics and its Applications*, **344**: 671–676, 2004.

[28] N. Laskin. Fractional market dynamics. *Physica A: Statistical Mechanics and its Applications*, **287**: 482–492, 2000.

[29] X. Li. Fractional differential equations and stable distributions. Department of Applied Mathematics, University of Western Ontario, London, Ontario, Canada N6A 5B7, 2003.

[30] Y. Lin and C. Xu. Finite difference/spectral approximations for the time-fractional diffusion equation. *Journal of Computational Physics*, **225**: 1533–1552, 2007.

[31] A. Loverro. Fractional calculus: History, definitions and applications for the engineer. USA: Department of Aerospace and Mechanical Engineering, University of Notre Dame, 2004.

[32] V. McGahay. Inertial effects and diffusion. *Journal of Non-Crystalline Solids*, **349**: 234–241, 2004.

[33] M. M. Meerschaert and E. Scalas. Coupled continuous time random walks in finance. *Physica A*, **370**: 114–118, 2006.

[34] M. M. Meerschaert and C. Tadjeran. Finite difference approximations for fractional advection-dispersion flow equations. *Journal of Computational and Applied Mathematics*, **172**: 65–77, 2004.

[35] R. Metzler and T. F. Nonnenmacher. Fractional diffusion, waiting-time distributions, and cattaneo-type equations. *Physical Review E*, **57**: 6409–6414, 1998.

[36] S. Momani. An algorithm for solving the fractional convection-diffusion equation with nonlinear source term. *Comunications in Nonlinear Science and Numerical Simulation*, **12**: 1283–1290, 2007.

[37] S. Momani and Z. Odibat. A novel method for nonlinear fractional partial differential equations: Combination of DTM and generalized Taylors formula. *Journal of Computational and Applied Mathematics*, **220**: 85–95, 2008.

[38] Z. Odibat and S. Momani. Numerical methods for nonlinear partial differential equations of fractional order. *Applied Mathematical Modelling*, **32**: 28–39, 2008.

[39] P. Carr, H. Geman, D. B. Madan and M. Yor. The fine structure of asset returns: An empirical investigation. *Journal of Business*, **75**: 305–332, 2002.

[40] I. Podlubny. Geometric and physical interpretation of fractional integration and fractional differentiation. *Fractional Calculus and Applied Analysis: An International Journal for Theory and Applications*, **5**: 367–386, 2002.

[41] R. L. Burden and J. D. Faires. *Numerical Analysis*. Brooks/Cole, Belmont, 2001.

[42] R. Metzler, J. Klafter and I. M. Sokolov. Anomalous transport in external fields: Continuous time random walks and fractional diffusion equations extended. *Physical Review E*, **58**: 1621–1633, 1998.

[43] T. Sottinen and E. Valkeila. On arbitrage and replication in the fractional Black-Scholes pricing model. *Statistics and Decisions*, **21**: 93–107, 2003.

[44] V. E. Lynch, B. A. Carreras, D. del-Castillo-Negrete, K. M. Ferreira-Mejias and H. R. Hicks. Numerical methods for the solution of partial differential equations of fractional order. *Journal of Computational Physics*, **192**: 406–421, 2003.

[45] V. S. Erturk, S. Momani and Z. Odibat. Application of generalized differential transform method to multi-order fractional differential equations. *Communications in Nonlinear Science and Numerical Simulation*, **13**: 1642–1654, 2008.

[46] A. Wazwaz and S. M. El-Sayed. A new modification of the Adomian decomposition method for linear and nonlinear operators. *Applied Mathematics and Computation*, **122**: 393–405, 2001.

[47] L. Yuan and O. P. Agrawal. A numerical scheme for dynamic systems containing fractional derivatives. *Journal of Vibration and Acoustics*, **124**: 321–324, 2002.

[48] S. B. Yuste and L. Acedo. An Explicit Finite Difference Method and a new Von Neumann-Type Stability Analysis for Fractional Diffusion Equations. *SIAM Journal on Numerical Analysis*, **42**: 1862–1874, 2005.

[49] L. Zhou and H. M. Selim. Application of the fractional advection-dispersion equation in porous media. *Soil Science Society of America Journal*, **67**: 1079–1084, 2003.